AN INVESTIGATION OF THE ELEVATOR AND RUDDER HINGE MOMENT PARAMETERS OF AN AIRCRAFT OBTAINED BY ANALYTICAL, WIND TUNNEL AND FLIGHT TEST DETERMINATION

JOHN S. McNULTY
ROBERT N. SMITH
NICHOLAS J. VAGIANOS

AN INVESTIGATION OF THE ELEVATOR AND RUDDER HINGE MOMENT PARAMETERS OF AN AIRCRAFT OBTAINED BY ANALYTICAL, WIND TUNNEL AND FLIGHT TEST DETERMINATION

by

Major John S. McNulty, USMC
Major Robert N. Smith, USMC
Lt. Nicholas J. Vagianos, USN

Aeronautical Engineering Report No. 421

Submitted in partial fulfillment of the requirements for the Degree of Master of Science in Engineering from Princeton University, 1958.

ACKNOWLEDGMENTS

The authors wish to express their appreciation to Professor Courtland D. Perkins, under whose supervision and guidance this investigation was carried out, and to Princeton University for the equipment and facilities provided at the Forrestal Research Center.

The authors also express their appreciation to Mr. Thomas E. Sweeney, whose valuable assistance and advice contributed materially to the timely completion of the wind tunnel and flight test phases of this report; and to Mr. R. F. Lehnert and staff for their assistance in the wind tunnel phase and the construction of the Navion model.

Thanks are also extended to Mr. Robert F. Cooper and the hangar staff for their assistance in aircraft instrumentation and maintenance of the test aircraft during this program.

TABLE OF CONTENTS

LIST OF TABLES

LIST OF FIGURES

SYMBOLS AND CONVENTIONS

AR	aspect ratio
a.c.	aerodynamic center
a	slope of lift curve
b	wing span (ft.)
c	chord (ft.)
C_h	hinge moment coefficient
$C_{h\alpha}$	$\partial C_h / \partial \alpha_t$
$C_{h\beta}$	$\partial C_h / \partial \beta$
$C_{h\delta}$	$\partial C_h / \partial \delta$
$C_{h\Psi}$	$\partial C_h / \partial \Psi = -C_{h\beta}$ in wind tunnel tests
C_L	lift coefficient
F_s	stick force (lbs)
G	gearing ratio (rad./ ft.)
H.M.	hinge moment (ft.lb.)
i	incidence (degrees)
K	constant = $-G\ S_e C_e \eta_t$ (rad. $ft.^2$)
l_t	tail length (distance from aircraft c.g. to a.c. of tail, ft.)
P.F.	rudder pedal force (lbs.)
q	dynamic pressure (psf)
S	wing area (sq. ft.)
V	velocity (mph)
W	average gross weight of aircraft (lbs.)

Greek Terms

α	angle of attack
β	sideslip angle
δ	angle of control surface deflection
ϵ	downwash angle
η_t	tail efficiency factor
ρ	density of air (slugs per cubic ft.)
λ	taper ratio
τ	elevator effectiveness
ϕ	trailing edge angle
$\frac{d\epsilon}{d\alpha}$	rate of change of downwash with angle of attack

Subscripts

c	calibrated
e	elevator
i	indicated
r	rudder
t	tail, tab
v	vertical tail
w	wing

SUMMARY

This investigation was conducted to determine the accuracy with which it was possible to predict the flight hinge moment derivatives of the elevator and rudder of a light subsonic airplane, using both analytical and wind tunnel methods. The hinge moment derivatives studied were those for the North American Navion N91566. The tests were conducted at the Forrestal Research Center of Princeton University, Princeton, New Jersey.

The values of the elevator hinge moment derivatives obtained analytically, from the wind tunnel, and by flight testing were in excellent agreement. The rudder derivatives obtained by flight testing were slightly larger than the other methods. This was partially due to the difficulty in producing large amounts of sideslip, and difficulty in accurate scaling of rudder in the model.

RESULTS

The results of the hinge moments investigation are shown in the following table:

	Elevator		Rudder	
	$C_{h_{\delta_e}}$	C_{h_α}	$C_{h_{\delta_r}}$	C_{h_β}
1 Analytical (thin airfoil theory)	-.0147	-.0073	-.0131	+.0058
2 Semianalytical-empirical	-.0092	-.0040	-.0120	+.0045
3 Wind tunnel (without spoiler wires)	-.0134	-.0043	-.0080	+.0039
4 Wind tunnel (with spoiler wires)	-.0105	-.0030	-.0070	+.0041
5 Flight test	-.0090	-.0040	-.0160	+.0070

The derivatives on line 1 were based on thin airfoil theory, corrected only for three-dimensional flow and neglecting other modifying effects, all of which tend to lower the values. These derivatives can be considered to be an upper limit as the physical airfoil approaches the theoretical thin airfoil.

Line 2 shows the results of a more exact semianalytical-empirical method which includes all modifying effects such as three-dimensional flow, section thickness, hinge gap spacing, flap leading edge shape, horns and Reynolds number. Since all these factors reduce the absolute value of hinge moments, the results on line 2 are lower than line 1.

The results given on lines 3 and 4 are for the wind tunnel model, run first without and then with 1/16-inch diameter spoiler wires on the stabilizer surfaces. The wires were placed at the 7 or 25 percent chord positions and

used to force a turbulent boundary layer. The results using the transition wires were considered more representative of full scale conditions.

The results on line 5 were obtained from flight test. The elevator derivatives were in fairly close agreement with the wind tunnel results, and in excellent agreement with the semianalytical-empirical method. However, there was less correlation in the rudder results. The rudder derivatives obtained by flight test were larger than any of the methods predicted. This may be partially due to a low order of accuracy of the actual rudder hinge moment flight test due to the difficulty in producing large amounts of side-slip with the two-foot chute used for this purpose.

A more thorough discussion of the results is presented in the Discussion section of this report.

AN INVESTIGATION OF THE ELEVATOR AND RUDDER HINGE MOMENT PARAMETERS OF AN AIRCRAFT OBTAINED BY ANALYTICAL, WIND TUNNEL AND FLIGHT TEST DETERMINATION

INTRODUCTION

It was desired to investigate the accuracy with which it was possible to predict the hinge moment derivatives of the tail of a light subsonic airplane by both analytical and wind tunnel means. The airplane upon which this investigation was performed was the North American Navion, whose normal speed range is approximately 80 to 150 miles per hour. The airplane characteristics are listed in Table I.

The hinge moment derivatives were predicted analytically by two methods. The first was based on thin airfoil theory, which neglected nearly all modifying effects such as thickness, hinge gap, elevator leading edge shape, the presence of elevator balancing horns, and the Reynolds number of the air. Three-dimensional effects, however, were taken into account. This simplified analysis was, therefore, expected to overestimate the derivatives on the high side. The second method was a semianalytical-empirical method using wind tunnel data published by the NACA. This data was then corrected for the geometry of the Navion tail.

The derivatives were also determined through wind tunnel tests of an 8:1 scale model of the Navion tail mounted on a streamlined shape, Fig. 12. The wind tunnel used for testing the model was the two- by three-foot test

section of the Subsonic Instructional Wind Tunnel at the Forrestal Research Center of Princeton University. The results from wind tunnel testing for hinge moments are subject to many possible errors, such as wind tunnel wall effects, inaccurate simulation of boundary layer conditions, inaccuracies in model geometry, and friction in the moment measuring devices. Considerable care was taken to minimize these errors in an attempt to obtain maximum accuracy.

The actual Navion was finally instrumented to obtain the full scale hinge moment data, and the full scale data developed from the appropriate flight tests.

From a comparison of the results, it was hoped to be able to determine the degree of reliability offered by the analytical and wind tunnel methods for predicting control hinge moments in low subsonic flow.

This analysis was conducted during the Spring semester of 1958 at the Forrestal Research Center of Princeton University, Princeton, New Jersey.

ANALYTICAL DEVELOPMENT

The analytical derivation of the hinge moment coefficients was accomplished by two methods. The first was a method based on thin airfoil theory and the second a semianalytical-empirical method using published section data and correcting the values for the Navion physical tail characteristics as given in Table I.

The first method is one derived in Ref. 1 from thin airfoil theory and is based wholly upon first order approximations. The theory completely neglects airfoil thickness, hinge gap, elevator leading edge shape, the presence of elevator or rudder horns, and the viscosity of the air. Three-dimensional effects were, however, accounted for. The resulting hinge moments, therefore, were expected to be of larger magnitude but the method was included in the analysis to show quantitatively the magnitude of errors involved when the modifying factors are neglected.

The expression for elevator hinge moment as given by Ref. 1 is:

$$M_h = 4\rho V^2 a^2 (\eta_1 \alpha + \eta_2 \delta)$$

where $\eta_1 = f(c_{h_\alpha})$

$\eta_2 = f(c_{h_\delta})$

and "a" is the radius of the transforming circle and is approximately equal to one-fourth the chord of the airfoil.

For control flaps where the ratios of flap chord to airfoil chord are not small, the parameters η_1 and η_2 are given below:

$$\eta_1 = -\epsilon_o + \sin\epsilon_o \cos\epsilon_o + 2\sin\epsilon_o - 2\epsilon_o \cos\epsilon_o$$

$$\eta_2 = \frac{1}{\pi}\left[\epsilon_o^2 + 2\epsilon_o^2 \cos\epsilon_o - 2\epsilon_o \sin\epsilon_o - \sin^2\epsilon_o\right]$$

The angle ϵ_o is shown in Fig. 2 and for an airfoil where the ratio of flap chord aft of the hinge line to airfoil chord is 35 percent, the value of ϵ_o is $72^o\ 32.5'$ or 1.266 radians. Substituting this value of ϵ_o into the previous two equations, gave the following values for η_1 and η_2:

$$\eta_1 = +0.1684$$

$$\eta_2 = -0.2423$$

The relations between η_1, η_2 and c_{h_α}, c_{h_δ} respectively were obtained by comparing similar terms of the two moment equations:

$$M_h = 4\rho V^2 a^2 (\eta_1 \alpha + \eta_2 \delta) = 1/2\,\rho V^2 S_e c_e (c_{h_\alpha}\alpha + c_{h_\delta}\delta)$$

where for the left side of the equation:

$$a = c/4$$

$$c_e = .35c$$

thus $$a^2 = \frac{c_e^2}{.1225}\,\frac{1}{16} = \frac{c_e^2}{1.96}$$

and for the right side of the equation:

$S_e = c_e \times 1$ for the area of airfoil per unit span.

Substituting the above values in the equations for the hinge moments, the hinge moment derivatives were obtained:

$$c_{h_\alpha} = \frac{\eta_1}{.245} = \frac{.16843}{.245} = +0.6875 \text{ per radian}$$

$$= +0.012 \text{ per degree}$$

$$c_{h_\delta} = \frac{\eta_2}{.245} = \frac{-.2423}{.245} = -0.9885 \text{ per radian}$$

$$= -0.0172 \text{ per degree}$$

Using the normal sign convention of downward elevator deflections being positive, Fig. 1, the sign of c_{h_α} becomes negative. The final two-dimensional derivatives were:

$$c_{h_\alpha} = -0.012 \text{ per degree}$$

$$c_{h_\delta} = -0.017 \text{ per degree}$$

These two-dimensional hinge moment derivatives were than corrected to three-dimensional flow using expressions derived from lifting line theory:

$$C_{h_\alpha} = c_{h_\alpha} \frac{a_t}{a_o} = c_{h_\alpha} \frac{C_{L_\alpha}}{c_{l_\alpha}}$$

$$C_{h_\delta} = c_{h_\delta} + \tau \left(C_{h_\alpha} - c_{h_\alpha} \right)$$

The three-dimensional slope of the lift curve for the horizontal tail was obtained from Fig. 5-5 of Ref. 2 with the aspect ratio of 4.03. The lift slope a_t obtained was .057/ degree. The three-dimensional elevator effectiveness, τ , was obtained from Fig. 5-33 of Ref. 2 by entering with the area ratio S_e / S_t:

$$\frac{S_e}{S_t} = \frac{14.098}{43.051} = 0.3275$$

The elevator effectiveness, τ , obtained was 0.53. These values of a_o and τ were then used in the above equations:

$$C_{h_\alpha} = -.012 \frac{.057}{.094} = -.0073$$

$$C_{h_\delta} = -.0172 + .53 (-.0073 + .012) = -.0147$$

The final results for the elevator corrected to three-dimensional flow were:

C_{h_α} = -.0073 per degree

C_{h_δ} = -.0147 per degree

The hinge moment derivatives for the rudder were also computed by the method based on thin airfoil theory. In this case the rudder chord was not a constant percentage of the total vertical tail chord. At the top, the rudder was 42.6 percent chord, and at the horizontal tail centerline, it was 36.92 percent. An arithmetic average of 39.76 percent chord was assumed as a mean aerodynamic chord. For a 39.76 percent chord, the angle θ_o was found to be 78.10 degrees or 1.364 radians. The parameters η_1 and η_2 were found to be:

η_1 = 0.235

η_2 = -0.320

For the rudder:

$$c_e = 0.398\, c \quad \text{and} \quad a = \frac{c}{4}$$

thus $$a^2 = \frac{c_e^2}{0.158} \frac{1}{16} = \frac{c_e^2}{2.529}$$

Therefore, the hinge moment derivatives for the rudder were obtained as follows:

$$c_{h_\alpha} = \frac{\eta_1}{0.316} = \frac{0.235}{0.316} = 0.743 \text{ per radian}$$

$$= 0.013/\text{degree}$$

$$c_{h_\delta} = \frac{\eta_2}{0.316} = \frac{-0.320}{0.316} = -1.013 \text{ per radian}$$

$$= 0.018/\text{degree}$$

Converting to rudder nomenclature the rudder derivatives became:

$$c_{h_\beta} = +0.013 \text{ per degree}$$

$$c_{h_\delta} = -0.018 \text{ per degree}$$

The rudder derivatives were also corrected for three-dimensional flow. Using an area ratio $S_r/S_{vt} = 0.469$ to enter Fig. 5-33 of Ref. 2, a $\tau = 0.64$ was obtained. The slope of the lift curve for the rudder was obtained using formula 8-19 in Ref. 2 to obtain the effective aspect ratio of the vertical tail:

$$ARe = 1.55 \frac{b_v^2}{S_v} = 1.55 \frac{(4.02)^2}{12.925} = 1.943$$

From Fig. 8-8 of Ref. 2 the slope of the lift curve was found to be:

$$a_{vt} = 0.043$$

The three-dimensional derivatives were then computed as follows:

$$C_{h_\beta} = c_{h_\beta} \frac{C_{y\beta}}{c_{y\beta}} = .013 \frac{.043}{.0955} = .0058$$

$$C_{h_{\delta_r}} = c_{h_{\delta_r}} + \tau \left[-C_{h_\beta} - (-c_{h_\beta}) \right]$$

$$= -.018 + .64 \, (-.0058 + .013)$$

$$= -.0131$$

The final results for the rudder corrected to three-dimensional flow were:

$$C_{h_\beta} = + 0.0058 \text{ per degree}$$

$$C_{h_{\delta_r}} = - 0.0131 \text{ per degree}$$

The second method was the semianalytical-empirical method. Since section data for the Navion tail sections were not available, it was necessary to use empirical data for sections that closely resembled the Navion tail sections and then apply corrections to obtain the final results. This was done by two different procedures for comparison, since there is no one procedure that is independent of assumptions.

The first procedure was to take the section hinge moment parameters for the NACA 0009 airfoil with a 30 percent chord flap and .005 c gap from Fig. 3. For a percent balance overhang c_b/c_f of 10.7 percent:

$$c_{h_\alpha} = -0.0065$$

$$c_{h_\delta} = -0.0112$$

$$\tau = -\alpha_\delta = +0.62$$

$$a_o = c_{l_\alpha} = 0.094$$

$$\phi = 11 \text{ degrees}$$

The hinge moment derivatives were then corrected to an airfoil with a 35 percent chord flap using Fig. 7. The following ratios were obtained:

$$\frac{c_e}{c} = 0.35 \qquad c_{h_\alpha} = -0.0089 \qquad c_{h_\delta} = -0.0138$$

$$\frac{c_e}{c} = 0.30 \qquad c_{h_\alpha} = -0.0075 \qquad c_{h_\delta} = -0.0130$$

Ratios

$$c_{h_\alpha} = \frac{89}{75} = 1.187$$

$$c_{h_\delta} = \frac{138}{130} = 1.062$$

Multiplying by the ratios to get c_{h_α} and c_{h_δ} for $0.35\ \frac{c_e}{c}$:

$$c_{h_\alpha} = (-0.0065)\ 1.187 = -0.0077$$

$$c_{h_\delta} = (-0.0112)\ 1.062 = -0.0119$$

Since the variation in the hinge moment parameters with airfoil section arises mostly as a function of the included angle at the section trailing edge, the following equations were used from Ref. 3, page 5, to correct data to the Navion tail trailing edge:

$$\Delta c_{h_\alpha} = 0.005\ a_o\ \Delta\phi$$

$$\Delta c_{h_\delta} = 0.0078\ a_o\ \tau\ \Delta\phi$$

Although the included angle for the NACA 0012 section is 15 degrees, the Navion tail measured only 13.5 degrees, due to having flat sided elevator

surfaces. Therefore, $\Delta\phi$ was equal to 2.5 degrees compared with ϕ = 11 degrees for the NACA 0009 section.

$$\Delta c_{h_\alpha} = 0.005\ (0.094)(2.5) = 0.0012$$

$$\Delta c_{h_\delta} = 0.0078\ (0.094)(0.62)(2.5) = 0.0011$$

Applying the above correction in the sense that larger included angles increase the derivatives positively:

$$c_{h_\alpha} = -0.0077 + 0.0012 = -0.0065$$

$$c_{h_\delta} = -0.0120 + 0.0011 = -0.0108$$

The three-dimensional flow corrections were the same as those used in the thin airfoil method for the elevator.

$$C_{h_\alpha} = c_{h_\alpha} \frac{a_t}{a_o} = c_{h_\alpha} \frac{C_{L_\alpha}}{c_{l_\alpha}}$$

$$C_{h_\delta} = c_{h_\delta} + \tau\,(C_{h_\alpha} - c_{h_\alpha})$$

Evaluating these expressions:

$$C_{h_\alpha} = -0.0065 \left(\frac{0.057}{0.094}\right) = -0.0040$$

$$C_{h_\delta} = -0.0108 + 0.53\ \left[-0.0040 - (-0.0065)\right]$$

$$= -0.0094$$

Since the elevator is equipped with horn balances, the hinge moment derivatives must be corrected for the decreasing effect of the horns. This was done using Fig. 8 entering the plot with the ratio:

$$\frac{\text{Area horn} \times \text{mean chord of horn}}{\text{Area of control} \times \text{mean chord of control}} = \frac{(0.1613)(0.646)}{(7.05)(1.28)}$$

$$= \frac{0.1042}{9.02} = 0.0155$$

The ΔC_{h_α} value was insignificant but the ΔC_{h_δ} value was $+0.0002$. Applying this correction, the final results for the three-dimensional hinge moment derivatives were:

$$C_{h_\alpha} = -.0040$$

$$C_{h_\delta} = -.0092$$

The second procedure used in the semianalytical-empirical method consisted of taking the hinge moment derivatives for the NACA 0009 and 0015 airfoil sections, since data for the NACA 0012 airfoil were not available. This data was for a 30 percent chord flap, a hinge gap of $0.005c$ and a $0.107c$ overhang of the elevator ahead of the hinge line. The value of $0.107c$ was selected as the average value along the span of the elevator. The values were obtained from Figs. 3 and 4 and were as follows:

	NACA 0009	NACA 0015
c_{h_α}	-0.0063	-0.0019
c_{h_δ}	-0.0112	-0.0054
c_{l_α}	0.094	0.092
$\tau = \alpha\delta$	0.62	0.48
ϕ	11°	19°

A linear variation of the parameters was assumed between the 0009 and 0015 sections and the following values were obtained for the NACA 0012 section:

$$c_{h_\alpha} = -0.0041$$

$$c_{h_\delta} = -0.0083$$

$$c_{l_\alpha} = 0.093$$

$$\alpha_\delta = 0.55$$

$$\phi = 15^\circ \text{ (actually measured as } 13.5^\circ)$$

The trailing edge included angle was measured to be 13.5° since the elevator surfaces are flat sided.

The derivatives c_{h_α} and c_{h_δ} were then corrected to a 35 percent chord elevator using Fig. 5 and the following values were obtained:

$$c_{h_\alpha} = -0.0052$$

$$c_{h_\delta} = -0.0090$$

The derivatives were then corrected for the difference of trailing edge included angles which was 1.5 degrees. The corrections were:

$$\Delta c_{h_\alpha} = 0.005\,(0.093)\,(1.5) = 0.0007$$

$$\Delta c_{h_\delta} = 0.0078\,(0.093)\,(0.62)\,(1.5) = 0.0007$$

and applied so as to increase the hinge moments negatively, since the trailing edge angle was corrected to a smaller value. The corrected two-dimensional hinge moment derivatives were:

$$c_{h_\alpha} = -0.0059$$

$$c_{h_\delta} = -0.0097$$

The derivatives were corrected to three-dimensional flow by using the same expression as was used in the previous procedures:

$$C_{h_\alpha} = c_{h_\alpha} \frac{C_{L_\alpha}}{c_{l_\alpha}}$$

$$C_{h_\delta} = c_{h_\delta} + \tau \left(C_{h_\alpha} - c_{h_\alpha} \right)$$

Inserting the numerical values:

$$C_{h_\alpha} = -.0059 \left(\frac{0.057}{0.093} \right) = -0.0036$$

$$C_{h_\delta} = -.0097 + 0.55 \left[-0.0036 - (-.0059) \right]$$

$$= -.0084$$

Applying the horn balance correction of $\Delta C_{h_\delta} = 0.0002$, the final three-dimensional hinge moment derivatives were:

$$C_{h_\alpha} = -0.0036$$

$$C_{h_\delta} = -0.0081$$

This method gave results approximately 10 percent lower than by the previous method.

The hinge moment derivatives for the rudder were calculated by the first procedure. The rudder does not have the simple geometric relationships that the elevator has; therefore, it was necessary to take average values for the section characteristics.

The vertical tail characteristics at the top plane of the rudder were as follows:

Airfoil section	NACA 0012.04 Mod
Airfoil chord (not modified)	19.779"
Rudder % chord (not modified)	28.9 %
Airfoil chord (modified)	24.669"
Rudder % chord (mqdified)	42.9 %
Percent overhang to rudder chord	5.63 %
Rudder chord	10.6"
Included angle at trailing edge	8.8°

The characteristics of the vertical tail at the bottom hinge of the rudder were as follows:

Airfoil section	NACA 0013.2 Mod
Extended airfoil chord (not modified)	47.23"
Rudder % chord (not modified)	29.75%
Extended airfoil chord (modified)	53.45"
Rudder % chord (modified)	37.07%
Percent overhand to rudder chord	6.69%
Rudder chord	19.8"
Included angle at trailing edge	10.3°

The section characteristics for the rudder were estimated as the arithmetic mean of the rudder top and bottom sections. The resulting values obtained were:

Airfoil section	NACA 0012.5 Mod
Airfoil chord	39.057"
Rudder % chord	39.99 %
Percent overhang to rudder chord	$\frac{c_b}{c_f}$ = 6.16 %
Rudder chord	15.2 "
Included angle at trailing edge	9.05°

The section hinge moment parameters for this averaged section obtained from Fig. 3 were as follows:

c_{h_α} = -0.0068

c_{h_δ} = -0.0130

$\tau = \alpha_\delta$ = +0.608

c_{l_α} = 0.095

ϕ = 11°

The hinge moments derivatives corrected to an airfoil with a 39.985 percent chord flap using Fig. 7 were:

$\frac{c_e}{c}$ = 0.40

c_{h_α} = -0.0101

c_{h_δ} = -0.0145

$\frac{c_e}{c}$ = 0.30

c_{h_α} = -0.0075

c_{h_δ} = -0.0130

Ratios

$$c_{h_\alpha} = \frac{107}{75} = 1.347$$

$$c_{h_\delta} = \frac{145.5}{130} = 1.119$$

Multiplying by the ratios

$$c_{h_\alpha} = (1.347)(-0.0067) = -0.0091$$

$$c_{h_\delta} = (1.119)(-0.0130) = -0.0145$$

Correcting for the trailing edge included angle:

$$\Delta c_{h_\alpha} = 0.005\ a_o\ \Delta\phi$$

$$= 0.005\ (0.095)(-1.95) = -0.0009$$

$$\Delta c_{h_\delta} = 0.0078\ a_o\ \tau\ \Delta\phi$$

$$= 0.0078\ (0.095)(0.608)(-0.95) = -0.0009$$

Applying the above corrections:

$$c_{h_\alpha} = -0.00910 - 0.0009 = -0.0100$$

$$c_{h_\delta} = -0.0145 - 0.0009 = -0.0154$$

The three-dimensional flow corrections were the same as those used in the thin airfoil method for the rudder.

The three-dimensional derivatives were derived as follows:

$$C_{h_\alpha} = c_{h_\alpha}\frac{a_v}{a_o} = (-.0100)\ \frac{.043}{.095} = -0.0045$$

$$C_{h_\delta} = c_{h_\delta} + \tau\ (C_{h_\alpha} - c_{h_\alpha})$$

$$= -.0154 + .64\ (-.0045 + .0100)$$

$$= -.0120$$

Rewriting the above using rudder nomenclature the results for the vertical tail were:

$$C_{h_\beta} = -C_{h_\alpha} = 0.0045$$

$$C_{h_{\delta_r}} = C_{h_\delta} = -0.0120$$

EQUIPMENT AND APPARATUS

Wind Tunnel and Wind Tunnel Model

The wind tunnel used for running the model was the 3-D side of the Subsonic Instructional Wind Tunnel located at the Forrestal Research Center of Princeton University. The test section of the 3-D side is a rectangular closed jet section, two feet in height and three feet in width. This side is capable of velocities up to approximately 97 miles per hour. (See Ref. 4 and Fig. 9.)

The wind tunnel model was an 8:1 scale model of the horizontal and vertical tail surfaces of the Navion, mounted on a streamlined shape. The streamlined shape retained the original fuselage cross-section characteristics for approximately two horizontal tail chord lengths and then faired into a rounded nose, as shown in Fig. 10. The elevator and rudder were hinged with ball bearing hinges to avoid any influence of hinge friction on the measured hinge moments.

The elevator could be set to any predetermined angle by the turning of a rod accessible at the nose of the streamlined body. The aft end of the rod was attached to a sliding mechanism upon which a small strain gage beam was attached. A link rod connected the other end of the beam to a lever arm inserted into the elevator hinge line shaft at the model center line, Fig. 12. Moments applied to the elevator were transmitted by the lever arm through the link rod to the strain gage beam where they were measured by the strain gage. By specifying a strain gage beam of as short a length as practical,

minimum deflections were encountered, which in turn kept elevator angle deviations to a minimum, as the aerodynamic loads were applied.

The rudder was controlled with a torque tube extending downward through the center of the turntable upon which the model supporting strut was fastened. A strain gage beam attached to a shaft at the lower end of the tube was calibrated to detect the rudder hinge moment. The rudder angle could be set by rotating the beam and tube to different angles and locking them at the desired angle, Fig. 11. Two universal bearings at each end of the tube permitted the rudder moment to be obtained at different angles of model pitch.

The model was mounted on a turntable of 27-inch diameter by a streamlined hollow steel strut of nine-inch length. The model had only freedom of pitch with respect to the supporting strut. Pitch was controlled by adjusting the length of a supporting turnbuckle attached between the after portion of the body and the turntable.

The model could be yawed about the rudder hinge line, by rotating the turntable. The rudder hinge line was vertical and passed directly through the center of the turntable when the model had a zero pitch angle. At any other pitch angle, the misalignment caused a tilt of the rudder hinge line, which was corrected by the universal bearings on either end of the torque tube.

The two strain gage beams were connected to a Carrier amplifier which provided the bridge circuit and balancing components for the strain

gages and, in addition, amplified the signal to provide the necessary sensitivity. The hinge moments were thus read in terms of microamperes on the meter attached to the amplifier and converted to moments by using the calibration data.

Aircraft Instrumentation:

The airplane used for the flight tests was a "Navion" manufactured by North American Aviation, Inc. This airplane is a four place, low wing monoplane, powered by a single Continental E 185, 205 horsepower engine. Fig. 19 and Fig. 20 show a three view drawing and photograph of the aircraft. The pilot stations are situated side by side and each is equipped with a set of rudder pedals and a control yoke. The two aft passenger seats were removed and a wooden platform installed to mount the necessary instrumentation components.

To obtain the required flight test data, it was necessary to be able to vary the center of gravity position and to provide a means of producing a variable amount of sideslip angle. It was also necessary to instrument the airplane so that it was possible to read stick force, elevator deflection, rudder pedal force, rudder deflection and sideslip angle.

The center of gravity was shifted fore and aft by using a sliding weight inside a tube. Basically, the system consisted of an 83 lb. 14.5 oz. cylinder of lead sliding in a 20-foot aluminum irrigation pipe of four-inch diameter. The movement of the weight was accomplished by means of a rachet arrange-

ment at the forward end of the tube driving a 3.5-inch sprocket over which ran a 1/8-inch bicycle chain. A similar sprocket was mounted at the rear of the tube and both ends of the chain were attached to the weight. Full travel of the weight produced a change of center of gravity of approximately nine percent m.a.c.

To produce the sideslip, a pilot chute from a standard Navy 28-foot parachute was used. The chute was attached to the right wing tip with a 10-foot nylon shroud line and a release mechanism which could be actuated from the cockpit. A second line was attached to the chute and led inside the fuselage through the exhaust port above the right wing root to an electric powered winch. The winch controlled the lateral position of the chute and, thereby, the amount of yawing moment required to produce sideslip. The chute, having a diameter of approximately two feet, produced a change in sideslip of approximately three degrees when the chute was moved from its full out to full in position. Although a larger change in sideslip was desirable from the standpoint of increased accuracy and could be obtained by using two chutes, it was not considered safe for take-off, since the take-offs were performed with the chute fully streamed. It was not possible to collapse the chute for take-off because the built-in spring designed into the chute prevented its being packed into a can.

The stick force was obtained by replacing the standard yoke by one which resembled an elongated "H", with the hub at the center of the cross

bar, Fig. 21. On each half of the cross bar were placed two strain gages. These measured the bending moments applied to the bars by the pilot's hands on the vertical members of "yoke handles." The strain gage circuit was so arranged as to yield the total force regardless of the distribution of forces on the two handles. The force indication was displayed on a microammeter. Since no amplifier was used due to weight and space limitations, it was necessary to design the required sensitivity of the meter indication into the system. The system was then calibrated with a spring scale. A calibration plot is shown in Fig. 29 and a wiring diagram of the circuit in Fig. 35.

The elevator deflection was obtained using a low friction potentiometer in the tail, which rotated with elevator movement, Fig. 24. Changing the potentiometer setting changed the reading of a microammeter in the cockpit. After proper calibration, it was possible to obtain elevator deflection. A calibration plot and wiring diagram are shown in Figs. 30 and 36 respectively.

The rudder pedal force was obtained by using a single cantilever beam mounted on the copilot's left rudder pedal and extending to the right. The beam had a bolt extending aft, perpendicular to the beam to insure a constant point of foot force application, Figs. 22 and 23. The strain gages, mounted on the beam, measured the bending in the beam. It was only necessary to have a beam on the left pedal, since the parachute on the right

wing tip always created negative sideslip, requiring left rudder to counteract it. A calibration plot and wiring diagram are shown in Figs. 31 and 37 respectively.

The rudder deflection was measured in the same manner as the elevator. A photograph of the potentiometer installation, a calibration plot, and wiring diagram are shown in Figs. 25, 32 and 38 respectively.

The sideslip angle was obtained by using a vane on a boom attached to the left wing tip, Fig. 27. The vane rotated a low friction potentiometer inside the boom which gave indications on a microammeter in the cockpit. Similar calibration procedures yielded the calibration plot in Fig. 33. The circuit diagram is shown in Fig. 39.

In order to insure accurate velocity measurements, the airspeed indicator was calibrated by making timed runs over a measured course. The airspeed calibration chart is shown in Fig. 34.

PROCEDURE

Wind Tunnel Testing

The model was tested in the 3D side of the Student Instructional Wind Tunnel at the Forrestal Research Center of Princeton University. The model was run at dynamic pressures as high as 24.1 pounds per square foot. This provided a Reynolds number of approximately 380,000 based on the horizontal tail chord, which was considerably lower than the 2,800,000 average at which the airplane flight tests were taken.

The equations used in reducing the data were derived from the hinge moment coefficient equation:

$$C_h = C_{h_\delta}\,\delta_e + C_{h_\alpha}\,\alpha = \frac{HM}{q\,S_e\,c_e}$$

where HM = hinge moment in foot-lbs

q = dynamic pressure in pounds per square foot

S_e = area of the elevator behind the hinge line

c_e = root mean square chord of the control surface aft of the hinge line

Taking the difference between two different δ_e and α positions, the following equations were obtained:

$$\Delta C_h = C_{h_\delta}\,\Delta\delta_{1\text{-}2} + C_{h_\alpha}\,\Delta\alpha_{1\text{-}2} = \frac{\Delta HM_{1\text{-}2}}{q\,S_e\,c_e}$$

Letting $\Delta\alpha_{1\text{-}2} = 0$, and solving for C_{h_δ}

$$C_{h_\delta} = \frac{\Delta HM_{1\text{-}2}}{q\,S_e\,c_e\,\Delta\delta_{1\text{-}2}}$$

Substituting in the appropriate conversion factors and dimensional values for the model:

$$C_{h_\delta} = \frac{-.0003215 \ \Delta \text{ grams}}{(.22028)(.14375)\ q\ \Delta\delta_e{}^o}$$

$$= \frac{-.010153}{q} \quad \frac{\Delta \text{ grams}}{\Delta\delta_e{}^o}$$

A similar derivation letting $\Delta\delta_{e_{1-2}} = 0$ produced the following equation for C_{h_δ}:

$$C_{h_\delta} = \frac{-.010153}{q} \quad \frac{\Delta \text{grams}}{\Delta\alpha^o}$$

Using the values for rudder area and chord

$S = .09456$ square feet

$c = .1583$ feet

the following equations were derived for the rudder:

$$C_{h_{\delta_r}} = \frac{-.0184}{q} \quad \frac{\Delta \text{grams}}{\Delta\delta_r{}^o}$$

$$C_{h_\beta} = \frac{+.0184}{q} \quad \frac{\Delta \text{grams}}{\Delta\beta^o}$$

The wind tunnel data obtained from the test runs were tabulated in Tables II through XVII. Wind tunnel wall corrections for change of induced angle of attack and streamline curvature were calculated as follows:

$$\alpha_{\text{final}} = \alpha_{\text{test}} + \Delta\alpha_i + \tau_2 \Delta\alpha_i$$

where $\Delta\alpha_i = \delta \frac{S}{C} C_L$

S = horizontal tail area

C = test section area

The value for δ was obtained from Fig. 6:30 of Ref. 5. Using $k = .4385$ for the horizontal stabilizer, δ was found to be 0.115. Therefore:

$$\Delta\alpha_i = 0.115 \frac{.6726}{5.814} = .0133$$

The value of τ_2 was obtained from Fig. 6:54 of Ref. 5 using lt/B of .03478. The value found for τ_2 was 0.10. The complete expression becomes:

$$\alpha_{final} = \alpha_{test} + .0133\ C_L + .00133\ C_L$$

$$\alpha_{final} = \alpha_{test} + .0146\ C_L$$

The corrections for the rudder were obtained in a similar manner. Using:

δ = .133

τ_2 = .08

S = .2018 square feet

C = 5.814 square feet

the following equation for the correction was derived:

$$\beta_{final} = \beta_{test} + .005\ C_L$$

Both these corrections were extremely small and would not alter the results; therefore, both were neglected. Had a larger model been used in the same test section, the corrections would have become more significant.

Amplifiers were used to amplify the signals from the resistance wire strain gage beams. The two systems were calibrated using weights acting on the control surfaces at a known distance from the hinge lines.

The elevator and rudder deflections could be read during the run in order that changes in deflections could be detected and recorded properly.

To force a turbulent boundar layer considered more typical of the full scale flight condition 1/16 inch wires were taped along the span of the horizontal and vertical stabilizers at seven percent chord for Runs II, IV, V and at 25 percent chord for Runs VI, IX, X, XV, XVI. Below is a diagram showing location of turbulence wires:

Wires at 7% chord Wires at 25% chord

Upon the completion of the testing, the model was removed and the test section was calibrated with a pitot static tube located at the centerline of the tunnel.

Flight Testing

The flight test procedure used to obtain the data for the elevator was the same as was employed in Ref. 6. The method is based on the following development.

Elevator Derivatives by Flight Test

C_{h_δ}:

The C_{h_δ} derivative for the elevator was obtained first. The total hinge moment coefficient of the elevator can be written as:

$$C_h = C_{h_\alpha} \alpha_t + C_{h_\delta} \delta_e + C_{h_{\delta_t}} \delta_t$$

If the airplane is flown in steady level flight and without changing the speed, power, or tab setting, the center of gravity is shifted in the longitudinal direction, a change in elevator angle and stick force will occur due to the change in lift now required from the horizontal tail to maintain level flight. The slight change of wing lift required, which results in a slight change in wing angle of attack and, thereby, tail angle of attack, $\Delta \alpha_t$, will be neglected. In addition, the tab was set at zero deflection on the ground and not changed during the flight tests, and changes of tab angle, $\Delta \delta_t$, were, therefore, zero. The tail efficiency η_t was assumed to be a constant, 1.0, over the speed range.

Writing the hinge moment coefficient expressions for two different center of gravity positions, and subtracting one from the other:

$$C_{h_1} = C_{h_\alpha} \alpha_{t_1} + C_{h_\delta} \delta_{e_1} + C_{h_{\delta_t}} \delta_{t_1}$$

$$C_{h_2} = C_{h_\alpha} \alpha_{t_2} + C_{h_\delta} \delta_{e_2} + C_{h_{\delta_t}} \delta_{t_2}$$

$$\Delta C_{h_{1-2}} = C_{h_\alpha} \Delta\alpha_{t_{1-2}} + C_{h_\delta} \Delta\delta_{e_{1-2}} + C_{h_{\delta_t}} \Delta\delta_{t_{1-2}}$$

Since $\Delta\alpha_{t_{1-2}}$ is essentially zero and $\Delta\delta_{t_{1-2}}$ is zero, the expression reduces to:

$$\Delta C_{h_{1-2}} = C_{h_\delta} \Delta\delta_{e_{1-2}}$$

The derivatives C_{h_δ} can then be expressed as:

$$C_{h_\delta} = \frac{\Delta C_{h_{1-2}}}{\Delta\delta_{e_{1-2}}}$$

The hinge moment coefficient can be found from the expression for stick force:

$$F_s = -G \cdot HM$$

$$= -G \left(C_h \, q \, S_e \, c_e \, \eta_t \right)$$

Solving for C_h

$$C_h = \frac{F_s}{-G \, q \, S_e \, c_e \, \eta_t}$$

The change in C_h is then given by:

$$\Delta C_{h_{1-2}} = \frac{\Delta F_{s_{1-2}}}{-G \, q \, S_e \, c_e \, \eta_t}$$

$$= \frac{-391 \left(F_{s_1} - F_{s_2} \right)}{G \, S_e \, c_e \, \eta_t \, V_{cal}^2}$$

Substituting the values for the Navion in the above equation, the expression for $\Delta C_{h_{1-2}}$ becomes:

$$\Delta C_{h_{1-2}} = \frac{-23.1}{V_{cal}^2} \left(F_{s_1} - F_{s_2} \right)$$

The equation for C_{h_δ} then becomes:

$$C_{h_\delta} = \frac{-23.1}{V_{cal}^2} \cdot \left[\frac{F_{s_1} - F_{s_2}}{\delta_{e_1}^o - \delta_{e_2}^o} \right]$$

Stick force and elevator deflections were recorded for two c.g. positions, the sliding weight full forward and full aft, for various speeds from 80 to 130 mph. The values were then substituted in the last equation and a plot of C_{h_δ} versus calibrated velocity was produce, Fig. 44.

C_{h_α}:

The C_{h_α} derivative was obtained next by flight testing. The derivation of the flight test procedure again depends on the difference of hinge moment coefficients at two different flight conditions. Rewriting the equation for change in total hinge moment coefficient:

$$\Delta C_{h_{1-2}} = C_{h_\alpha} \Delta \alpha_{t_{1-2}} + C_{h_\delta} \Delta \delta_{e_{1-2}} + C_{h_{\delta_t}} \Delta \delta_{t_{1-2}}$$

Again the trim tab was set and left at zero, making $\Delta \delta_{t_{1-2}} = 0$.

Solving the last equation for C_{h_α}:

$$C_{h_\alpha} = \frac{\Delta C_{h_{1-2}} - C_{h_\delta} \Delta \delta_{e_{1-2}}}{\Delta \alpha_{t_{1-2}}}$$

The flight testing was conducted by flying the airplane at a constant power setting, tab setting and center of gravity location. At one velocity, the stick force and elevator deflection were measured. The velocity was changed by going into a slight glide or climb and the new stick force and elevator deflection were recorded. This provided information from which C_{h_α} was evaluated at some average velocity, using the previous equation. In this case ΔC_h was calculated for two different velocities and was expressed as:

$$\Delta C_{h_{1-2}} = \frac{1}{-G\, S_e\, c_e\, \eta_t} \Delta \left(\frac{F_s}{q}\right)_{1-2}$$

$$= \frac{391}{-G\, S_e\, c_e\, \eta_t} \left[\frac{F_{s_1}}{V_{cal_1}^2} - \frac{F_{s_2}}{V_{cal_2}^2}\right]$$

Substituting into the last equation the values for the Navion, the expression for $\Delta C_{h_{1-2}}$ became:

$$\Delta C_{h_{1-2}} = -23.1 \left[\frac{F_{s_1}}{V_{cal_1}^2} - \frac{F_{s_2}}{V_{cal_2}^2}\right]$$

The expression for $\Delta \alpha_{t_{1-2}}$ was developed from the expression:

$$\alpha_t = \alpha_w - \epsilon + i_t - i_w$$

For a first approximation of the downwash at the tail, the downwash can be assumed to be the same as the theoretical value of the downwash at infinity:

$$\epsilon^o = \frac{114.6\ C_L}{\pi\ A}$$

Therefore the expression for α_t can be written as:

$$\alpha_t = \frac{d\alpha}{dC_L} C_L - \frac{d\epsilon}{dC_L} C_L + i_t - i_w$$

Since $C_L = \frac{W}{qS}$ and $\frac{d\epsilon}{dC_L} \pm \frac{114.6}{\Pi A}$ at the tail

$$\alpha_t = \frac{1}{a_w} \frac{W}{qS} - \frac{114.6}{\Pi A} \frac{W}{qS} + i_t - i_w$$

$$= \frac{W}{qS} \left(\frac{1}{a_w} - \frac{114.6}{\Pi A} \right) + i_t - i_w$$

The increment of α_t due to a change in velocity can then be expressed as:

$$\Delta\alpha_{t_{1-2}} = \frac{2W}{\rho_o S} \left(\frac{1}{a_w} - \frac{114.6}{\Pi A} \right) \left[\frac{1}{V_{cal_1}^2} - \frac{1}{V_{cal_2}^2} \right]$$

It was desired to use a more refined value of downwash and the method presented in Refs. 2 and 7 was used to determine a more accurate value of $d\epsilon / d\alpha$. Using the m and r parameters, Figs. 5-9 and 5-10 of Ref. 2 and the curves of Ref. 7:

$$m = \frac{\text{vertical dist. horiz. tail a.c. to zero lift line}}{\text{wing semi-span}}$$

$$r = \frac{\text{dist. root 1/4 chord to horiz. tail a.c.}}{\text{wing semi-span}}$$

For the Navion:

$$m = \frac{31/12}{16.7} = 0.16$$

$$r = 15/16.7 = 0.9$$

From Fig. 5-10, Ref. 2:

$$\frac{d\epsilon}{d\alpha} \quad (\text{for} \quad \lambda = 3{:}1) = 0.43$$

$$\frac{d\epsilon}{d\alpha} \quad (\text{for} \quad \lambda = 1{:}1) = 0.35$$

Interpolating for $\lambda = 2{:}1$ gave $d\epsilon / d\alpha = 0.39$ at the aircraft centerline. This was corrected for the tail span and wing span using Fig. 21 of Ref. 7:

$$\frac{b_t}{b_w} = 0.395 \text{ gave a correction factor of } 0.935$$

Therefore:

$$\frac{d\epsilon}{d\alpha} = (0.39)(0.935) = 0.365$$

and

$$\frac{d\epsilon}{dC_L} = \frac{d\epsilon}{d\alpha}\frac{d\alpha}{dC_L} = (0.365)\frac{1}{.097} = 3.76$$

Since the equation for $\Delta\alpha_{t_{1-2}}$ is of the form:

$$\Delta\alpha_{t_{1-2}} = \frac{391\,W}{S}\left[\frac{1}{a_w} - \frac{d\epsilon}{dC_L}\right]\left[\frac{1}{V_{cal_1}^2} - \frac{1}{V_{cal_2}^2}\right]$$

the value of 3.76 may be substituted in for the theoretical value of $d\epsilon / dC_L$. The final expression for $\Delta\alpha_{t_{1-2}}$ is then obtained:

$$\Delta\alpha_{t_{1-2}} = \frac{391\,W}{S}\left[\frac{1}{a_w} - 3.76\right]\left[\frac{1}{V_{cal_1}^2} - \frac{1}{V_{cal_2}^2}\right]$$

Substituting the physical characteristics for the Navion:

$$\Delta\alpha_{t_{1-2}} = 53,173.3\left[\frac{1}{V_{cal_1}^2} \quad \frac{1}{V_{cal_2}^2}\right]$$

The expression for C_{h_α} may now be written:

$$C_{h_\alpha} = \frac{-23.1\left[\frac{F_{s_1}}{V_{cal_1}^2} - \frac{F_{s_2}}{V_{cal_2}^2}\right] - C_{h_\delta}\ \delta_1^\circ - \delta_2^\circ}{53,173.3\left[\frac{1}{V_{cal_1}^2} - \frac{1}{V_{cal_2}^2}\right]}$$

Two methods of reducing the data for C_{h_α} were available. The first method was to substitute in the expression for C_{h_α} the flight test values and plot numberous values of C_{h_α} versus velocity. The second method was to make two plots, one of elevator deflection versus velocity, the other of stick force versus velocity, by recording values from numerous flight test runs. Both methods were investigated and it was found that a definite curve of elevator deflection versus velocity and also stick force versus velocity could be obtained. These curves are Figs. 40 and 41, respectively. From these smooth curves, differences of stick force and elevator deflection were obtained and substituted in the expression for C_{h_α} and a plot of C_{h_α} versus calibrated velocity constructed, Fig. 45. Due to the complexity of the expression for C_{h_α}, it was found that the value was very sensitive to the accuracy with which the numerical calculations were performed.

Data for both derivatives, C_{h_α} and C_{h_δ}, were obtained through the speed range of 80 to 130 mph indicated airspeed. The plots of $C_{h_{\delta_e}}$ and C_{h_α} versus calibrated velocity are shown in Figs. 44 and 45.

Rudder Derivatives by Flight Test

The flight procedures for the rudder hinge moment derivatives were comparatively easier to develop, since any of the variables controlling the total hinge moment coefficient could be made zero. By flying the airplane at a constant velocity and by varying the wing tip parachute to two different positions, two different rudder pedal forces and rudder deflections could be obtained.

The biggest problem to overcome in the flight testing for the rudder derivatives was a safe, efficient means of producing a steady sideslip. With a multi-engine airplane this can easily be accomplished by varying the power of the engines on opposite wings, but with a single engine airplane, sideslip must be produced by some other means. For this investigation it was decided to use a small, two-foot diameter parachute attached to the right wing tip, Figs. 26 and 28. The drag of the parachute at the wing tip acting on a lever arm of 16 feet was estimated to produce about four degrees of sideslip. The amount of sideslip could be decreased by pulling the parachute inboard, thus reducing the lever arm.

It was necessary to use a small electrically powered winch to control the chute position. A toggle switch for operating the winch was mounted on the flight test instrument console between the pilot and the observer. With this arrangement, the observer could more easily control the amount of sideslip while applying left rudder on the strain-gage rigged rudder pedal,

and observing the microammeters which indicated sideslip angle, rudder deflection, and rudder force.

The technique for obtaining data for C_{h_β} was to fly at 100 mph in smooth air at a constant altitude with a fixed power setting, 22.5 inches of manifold pressure and 2050 rpm. The pilot held the airplane in steady flight at 100 mph while the observer held a constant rudder deflection, using the strain-gage instrumented left rudder pedal. Simultaneous readings of sideslip angle, rudder deflection, and rudder force were recorded when the pilot called out that the airspeed was steady at 100 mph. Then the chute was pulled inboard, reducing the sideslip angle and rudder force as a constant rudder deflection was maintained. When the airspeed and the three microammeters were steady, the data were recorded again. This procedure was repeated for different rudder deflections.

C_{h_β}:

Writing the expression for the pedal force difference:

$$\Delta P.F. = -G \cdot \Delta HM = -G\, q\, S_r\, c_r\, \eta_t\, \Delta C_h = K\, q\, \Delta C_h$$

where $K = -G\, S_r\, c_r\, \eta_t$

Then $$\Delta P.F. = K\, q\, (C_{h_\beta}\, \Delta\beta + C_{h_\delta}\, \Delta\delta_r + C_{h_{\delta_t}}\, \Delta\delta_t)$$

Since the only rudder tab is a fixed tab, this makes $\Delta\delta_t = 0$.

Then solving for C_{h_β}:

$$C_{h_\beta} = \frac{\Delta P.F. - K\, q\, (C_{h_\delta}\, \Delta\delta_r)}{K\, q\, \Delta\beta}$$

In flight testing for C_{h_β}, the rudder deflection was made zero for each reading, therefore $\Delta \delta_r = 0$. The expression for C_{h_β} became:

$$C_{h_\beta} = \frac{\Delta P.F.}{K\, q\, \Delta \beta}$$

Substituting the appropriate physical characteristics for the Navion:

$G = 1.38$

$S_r = 6.21$ sq. ft.

$c_r = 1.27$ ft.

$\eta_t = 1.0$

the final expression for C_{h_β} became:

$$C_{h_\beta} = \frac{391\ \Delta P.F.}{(-11.0)\ V_{cal}^2\ \Delta \beta} = \frac{-35.6}{V_{cal}^2} \left[\frac{F_{r_1} - F_{r_2}}{\beta_1{}^\circ \quad \beta_2{}^\circ} \right]$$

where $P.F. = F_r =$ Rudder Pedal Force

$\underline{C_{h_{\delta_r}}}$:

The derivative $C_{h_{\delta_r}}$ was test flown by flying at one constant velocity and taking two readings of pedal force and rudder deflection by varying the chute position. In this case the aircraft was maintained at constant sideslip, that is $\Delta \beta = 0$, with the rudder. The expression for $C_{h_{\delta_r}}$ then became:

$$C_{h_{\delta_r}} = \frac{-35.6}{V_{cal}^2} \left[\frac{F_{r_1} - F_{r_2}}{\delta_{r_1}{}^\circ - \delta_{r_2}{}^\circ} \right]$$

Data for both derivatives, C_{h_β} and $C_{h_{\delta_r}}$, were obtained for the speed of 100 mph indicated velocity only, but at varying angles of sideslip and rudder deflection. It was felt that a better comparison of results could be made with the wind tunnel by this procedure than if the tests for the rudder were made at varying velocities. Also it was felt advisable to keep the velocity low to avoid the possibility of a chute failure.

It was found that the rudder force and rudder deflection were quite steady when flying in smooth air, but that the sideslip indicating vane was very sensitive to any disturbance. This became very important in taking the data for $C_{h_{\delta_r}}$ since these runs were made at constant sideslip, while varying rudder deflection and rudder forces as the parachute was moved from the full out position to the inboard position.

DISCUSSION

The results of the hinge moments investigation are shown in the following table:

		Elevator		Rudder	
		$C_{h_{\delta_e}}$	C_h	$C_{h_{\delta_r}}$	C_{h_β}
1	Analytical (thin airfoil theory)	-.0147	-.0073	-.0131	+.0058
2	Semianalytical-empirical	-.0092	-.0040	-.0120	+.0045
3	Wind tunnel (without spoiler wires)	-.0134	-.0043	-.0080	+.0039
4	Wind tunnel (with spoiler wires)	-.0105	-.0030	-.0070	+.0041
5	Flight test	-.0090	-.0040	-.0160	+.0070

The results on line 1 were based on thin airfoil theory and were corrected only for three-dimensional flow. All other effects were neglected. These include airfoil section thickness, hinge gap spacing, bluntness of the control flap leading edge, presence of balancing horns and turbulence of the boundary layer. Any increase in any of these factors tends to lower the absolute value of the hinge moments. The results on line 1, therefore, should represent the maximum hinge moments possible if the actual airfoil is made to approach the theoretical thin airfoil configuration.

The results on line 2 were based on experimental data published by the NACA in Refs. 3 and 8. All the factors which were neglected in the line 1 analysis were accounted for in line 2, and the results should be an accurate representation of the actual hinge moments. The values obtained

by this method are all smaller, by varying amounts, than the values obtained by the method of line 1.

The results on line 3 were obtained from the wind tunnel tests of the 8:1 scale model of the Navion tail. The derivatives C_{h_α} and C_{h_β} obtained from the wind tunnel tests were in excellent agreement with those obtained by the semianalytical-empirical method of line 2. However, the value of $C_{h_{\delta_e}}$ was 46 percent higher than the semianalytical and $C_{h_{\delta_r}}$ was 33 percent lower than the semianalytical.

Three major factors which may have accounted for the discrepancy between wind tunnel and theory are: 1) the difficulty encountered in attempting to maintain the proper gap spacing in a test model that has dimensions which are comparatively small; 2) the difficulty in accurately determining the slope of C_h versus the independent variables δ_e, α, δ_r, and β at the zero value of the variable; and 3) the difference in the Reynolds numbers at which the model data and the theory test data were obtained.

The NACA tests were based on chord lengths of approximately two feet, whereas the Navion model average chord was approximately five inches, and both tests were conducted at approximately the same dynamic pressure of 20 pounds per square foot. The Reynolds number difference was 1,500,000 for the NACA and 380,000 for the Navion model. Since the pressure distribution over the chord of the airfoil section changes with

Reynolds number in the low Reynolds number regime, a variance of hinge moment can be expected. See Ref. 9.

The results on line 4 were obtained from the wind tunnel using spanwise spoiler wires of 1/16-inch diameter, located on both the upper and lower surfaces of the horizontal stabilizer and on both sides of the rudder fin. Elevator Runs II, IV and V were made with the wire located on the horizontal stabilizer at seven percent chord and Run VI at 25 percent. Stall buffeting occurred at angles of attack larger than five degrees when the wire was located at seven percent chord. Moving the wires to 25 percent delayed separation until seven degrees angle of attack. Stalling drastically increased the derivative C_{h_α}, due to the lowering of the pressure on the upper surface caused by the wire induced flow separation. The rudder was affected similarly by the wire at 25 percent chord, except the stall buffet was delayed until 10 degrees. The delay in stall may have been aided by the dorsal fin.

For angles of attack and yaw below buffet, the wires, due to an increase in the boundary layer turbulence, caused a decrease in the derivatives $C_{h_{\delta_e}}$, C_{h_α} and $C_{h_{\delta_r}}$. The derivative C_{h_β} was not appreciably affected.

The wind tunnel results using the spoiler wires should give a closer agreement with the full scale airplane since the effect of the wires was to simulate an increase of Reynolds number. The wind tunnel model

was operated at a Reynolds number of approximately 380,000 and the airplane at 2,800,000. Therefore, the addition of the wires was desirable in attempting to duplicate the full scale conditions.

The results on line 5 were obtained by flight testing the Navion. Both elevator derivatives were in perfect agreement with the semianalytical-empirical values. $C_{h_{\delta_e}}$ was 15 percent lower than the wind tunnel test using spoiler wires, whereas C_{h_α} had a value between the two wind tunnel tests. However, the rudder derivatives by flight test were larger than the values obtained by all other methods.

Several factors contributed to the discrepancy in the results obtained for the rudder. First, the order of accuracy of the elevator flight tests was greater than that of the rudder. This is a direct result of being unable to create large enough yawing moments with the two-foot diameter chute. Small yawing moment changes, therefore, produced only small changes in the pedal force, rudder deflection and sideslip. With the pedal force points close together, any error in reading the pedal force microammeter or in converting to force by using the calibration chart, Fig. 31, created a drastic variance in the slopes of P.F. vs δ_r, Fig. 42, and P.F. vs β, Fig. 43. This caused the large scatter of points in Figs. 46 and 47, which lowered the accuracy of the final average hinge moment derivatives $C_{h_{\delta_r}}$ and C_{h_β} for the rudder.

Additional factors also contributed to the discrepance in results between the flight test and the semianalytical-empirical analysis. The analytical hinge moments may be lower than the flight test values because the proper effective trailing edge included angle was not taken into account. The rudder has a sheet metal fixed tab extending 1.4 inches aft and extends along approximately 1/3 of the length of the trailing edge. This tab may effectively reduce the included angle along that portion of the trailing edge and if taken into account would increase the analytical derivatives.

Another factor is the fact that it is very difficult to determine the effective aspect ratio, lift curve slope, and control effectiveness of the rudder, accurate knowledge of which is necessary in the analytical analyses.

The discrepancy between the flight test and wind tunnel results may have been caused by several factors. First, due to the small scale size of the model, the gap size was larger than that on the airplane, especially at the lower half of the rudder. Here, the gap was effectively increased by the cavity in which the rudder torque shaft was attached. In addition, the fuselage was wider than the rudder at the point where it faired into the rudder, creating the possibility of turbulence along the lower portion of the rudder. The supporting struts along the bottom of the fuselage would also create a turbulent wake which might act to lower the hinge moments of the rudder.

Another factor may have been the relative surface roughness. The airplane had a relatively smooth lacquer finish while the model was relatively rough. This would tend to decrease the wind tunnel derivatives.

A third factor may have been the difference in shape of the trim tab between the model and the airplane. Any difference here would change the effective trailing edge included angle. The difficulties encountered herein with respect to the model stems from the fact that the scale of the model was effectively too small to accurately reproduce the physical characteristics of the rudder. Despite the small scale size, the actual included angles for both the elevator and rudder were duplicated within a fraction of a degree.

It is apparent that if a higher order of accuracy is desired a model of such small dimensions is not completely satisfactory for obtaining hinge moment derivatives. It is recommended that a larger model be constructed, preferably not smaller than 3:1 scale, for a tail the size of the Navion. The model should be a duplicate copy of the full scale tail, and if possible, be manufactured by the shop which produces the full scale tail. Specifically, if the control surfaces are made of fabric, so should the model; and if the surfaces are made out of sheet metal, the model should be made of similar scaled down material. The importance of this lies in the fact that any bulging of the surfaces greatly affects the hinge moments. Normally, an increase in the thickness due to bulging will decrease the hinge moments.

Flight techniques, weather conditions, and airplane instrumentation are vitally important in obtaining accurate flight test data. Weather conditions must be such that the flight is flown in still air, away from clouds. It was found that the best data was obtained at night or in the early morning. The slightest amount of thermal activity rendered any data taken unreproduceable, and therefore useless, due to the large scatter in the data. Instrumentation must be such that readings can be taken with reasonable accuracy. Trying to read small deflections on a crowded meter scale is useless. It is strongly recommended, in any future testing of rudder hinge moments of single engine aircraft, that a larger sideslip producing parachute be used. The capability to produce at least five degree change of sideslip with the parachute is necessary to perform proper testing. A chute of this size would necessarily have to be contained in a container for take-off, streamed out during the test and jettisoned prior to landing. In addition, the capability of mounting chutes on either wing tip in order to produce right and left sideslip is necessary, if the slope of C_h vs β is to be obtained at zero sideslip.

The large scatter in the $C_{h_{\delta_r}}$ data is believed to be caused partially by the difficulty in maintaining a constant sideslip angle. The sideslip angle was extremely sensitive to any atmospheric disturbance or the slightest aileron displacement. A larger chute and, therefore, larger sideslip angles would tend to minimize this type of error.

Since the hinge moments for both the elevator and rudder were measured at the control stick and rudder pedal, any friction in the control system would introduce errors in the force readings, algebraically adding or subtracting depending upon which direction the control was last moved. In the case of the Navion, the friction in the control systems was estimated at approximately two pounds. Since this is not considered an excessive amount, reasonable data accuracy was obtained for the elevator by repeating runs several times and by using average values of control forces. This procedure thus largely eliminated the error due to friction. In the case of the rudder, small pedal force changes due to the small sideslip chute, allowed the friction to become significant, increasing scatter and possibly reducing the accuracy of the results.

The only factors affecting the hinge moments in this low speed investigation were boundary layer effects and physical dimensions. At higher speeds where compressibility and aeroelastic effects become significant the additional complications may increase the difficulty of predicting the hinge moment derivatives.

CONCLUSIONS AND RECOMMENDATIONS

In attempting to determine control surface hinge moments, a careful analysis must be made of all the variables affecting the hinge moments; and unless this is done, incorrect results will be obtained. An analytical calculation must, therefore, account for all these influencing factors in the form of corrections. A wind tunnel investigation must duplicate the actual model in all details, and flight conditions must be simulated as closely as possible. Flight tests must be conducted in perfectly smooth air, and instruments must be easy to read for satisfactory results.

In wind tunnel testing it is recommended that a large enough scale model be used to enable authentic duplication of the original, especially with respect to surface characteristics, trailing edge angles, the trailing edge itself, and the hinge gap size. It is extremely important to duplicate boundary layer conditions.

In flight testing, a data recording scheme would be superior to a visual reading of instruments. A larger chute, capable of producing at least five degrees of sideslip and mountable on either wing would increase data accuracy. A rapid means of changing the center of gravity location for the elevator derivatives, is a recommended convenience leading to increased efficiency and accuracy. Locking the trim tab at the required position by a positive external locking mechanism eliminates the tendency of the tab to deflect, thereby eliminating erroneous stick force data. Friction can be

eliminated by taking force measurements at the control surface, or if the friction is small, take repeated runs and average out the friction error.

REFERENCES AND BIBLIOGRAPHY

1. Durand, William F.: Aerodynamic Theory, A General Review of Progress, 1934, J. Springer, Berlin.

2. Perkins, Courtland D., and Hage, R. E.: Airplane Performance Stability and Control, 1949, John Wiley and Sons, New York, N. Y.

3. Crane, Robert M.: Computation of Hinge Moment Characteristics of Horizontal Tails from Section Data. NACA Wartime Rep. A-11, 1945.

4. Williams, Forman A., Carter, R., Landis, H., and Wilkinson, R.: Calibration of the Princeton University Subsonic Instructional Wind Tunnel. Princeton University Rep. 288, 1954.

5. Pope, Alan: Wind Tunnel Testing, 1954, 2nd Ed., John Wiley and Sons, New York, N. Y.

6. Horner, Richard E., and Butman, P. M.: A Flight Testing Method of Determining Elevator Hinge Moment Parameters Associated with Elevator Deflection, Trim Tab Deflection and Angle of Attack. Princeton University Rep. 113, 1947.

7. Silverstein, Abe, and Katzoff, S.: Design Charts for Predicting Downwash Angles and Wake Characteristics Behind Plain and Flapped Wings. NACA Rep. 648, 1939.

8. Sears, Richard I.: Wind Tunnel Data on the Aerodynamic Characteristics of Airplane Control Surfaces. NACA Wartime Rep. L-663, 1943.

9. Pinkerton, Robert M.: The Variation with Reynolds Number of Pressure Distribution Over an Airfoil Section. NACA Rep. 613, 1938.

Advisory Group for Aeronautical Research and Development Flight Test Manual, Volume II, Stability and Control, Edited by Perkins, Courtland D., Princeton University, 1954.

Advisory Group for Aeronautical Research and Development Flight Test Manual, Volume IV, Instrumentation Systems, Edited by Durbin, Enoch J., Princeton University, 1957.

Duncan, W. J.: The Principles of the Control and Stability of Aircraft, 1952, Cambridge University Press.

TABLE I

PHYSICAL CHARACTERISTICS OF NAVION

A. WING

1.	Total Wing Area, S_w (includes flaps, ailerons and 19.87 ft^2 covered by the fuselage)	184.34 ft^2
2.	Span, b_w	33.38 ft
3.	MAC	68.35 in.
4.	Angle of Incidence:	
	Root, i_r	$+2^o$
	Tip, i_t	-1^o
5.	Twist:	
	Aerodynamic	2^o 31'
	Geometric	3^o 00'
6.	Airfoil Section:	
	Root	NACA 4415R
	Tip	NACA 6410R
7.	Aspect Ratio, AR_w	6.044
8.	Taper Ratio, λ_w	0.526
9.	Dihedral	7.5^o
10.	Root Chord	7.2 ft
11.	Tip Chord	3.92 ft
12.	Zero lift line angle of attack	-1.7^o

B. HORIZONTAL TAIL

1.	Total Area (includes 2.368 ft^2 covered by fuselage)	43.05 ft^2
2.	Span, b_h	13.17 ft
3.	Airfoil Section	NACA 0012
4.	Taper Ratio, λ_t	.667
5.	MAC, c_t	3.34 ft
6.	Aspect Ratio	4.03
7.	Root Chord	48 in.
8.	Tip Chord	30.89 in.

B-1. HORIZONTAL STABILIZER

1.	Area, S_s	28.95 ft^2
2.	Tail incidence with respect to FRP	-3^o

TABLE I (Cont.)

PHYSICAL CHARACTERISTICS OF NAVION

B-2. ELEVATORS

(No Trailing Edge Extensions)	Smooth skin Flat sided No trim bungee Balance spring
1. Area (aft of hinge line) Both elevators	14.098 ft^2
2. Span (physical dimension of half elevator)	(6.132 ft (73.582 in.
3. Deflection, δ_e	30° Up; 20° Dn
4. Root Chord (aft of hinge line)	16.8 in.
5. Tip Chord (aft of hinge line)	10.81 in.
6. Elevator MAC	1.28
7. Root Mean Square Chord	1.15
8. Trim Tabs (two tabs, 6 x 32.5 in.)	
9. Elevator Gearing Ratio	1.0
10. ϕ (trailing edge included angle)	13.5°

C. VERTICAL TAIL

1. Total Area, S_V (includes 2.577 ft^2 blanketed by fuselage and excluding 1.483 ft^2 of dorsal fin)	12.925 ft^2
2. Airfoil Section: Root Tip	 NACA 0013.2 Mod. NACA 0012-64 Mod.

C-1. VERTICAL STABILIZER

1. Area, S_{V_S} (includes 0.1427 ft^2 blanketed by fuselage)	6.873 ft^2
2. α (with reference to fuselage G_L)	2° Nose Left

TABLE I (Cont.)

PHYSICAL CHARACTERISTICS OF NAVION

C-3. RUDDER

	(1.4 x 16.0 in. trailing edge extension)	Smooth skin Rigged 3 Rt to Fin G Fixed bend tab
1.	Area, S_r (aft of hinge line)	6.052 ft^2
2.	Rudder Deflection, δ_r	17° L; 23° R
3.	Rudder Pedal Throw	5.75 in.
4.	Trim Tab	Fixed bend tab
5.	Rudder Gearing Ratio	1.38
6.	ϕ at top of rudder	8.8°
7.	ϕ at bottom of rudder	10.3°
8.	Average Rudder Chord	15.2 in.

D. MISCELLANEOUS

1.	Tail Length (CG to AC of vertical tail), l_{vt}	16.88 ft
2.	Distance from Fuselage Center Line to Wing Tip Parachute Mount	16.00 ft
3.	Weight (including two pilots and 30 gal. fuel)	2620 lbs
4.	Wing Tip Parachute (diameter)	2.00 ft
	Area (effective)	1.73 ft^2
	Drag Coefficient (based on effective area)	1.7
5.	Dorsal Fin Area	1.483 ft^2
6.	Rudder Fixed Tab Area	.155 ft^2

TABLE II

NAVION TAIL WIND TUNNEL TEST

Run I: Elevator Hinge Moment Coefficients at Constant Angle of Attack

Date: 13 April 1958

1	2	3	4	5
α deg.	δ_e deg.	force grams	q psf	C_h .000421(col. 3)
0	0	- 21.4	24.122	- 0.90
	3.80	-126.0		- 5.31
	8.25	-262.0		-10.05
	12.25	-397.0		-16.70
	16.00	-589.0		-24.00
	19.90	-697.0		-29.35
	- 4.00	+ 72.0		+ 3.03
	- 8.00	225.0		9.47
	- 8.00	225.0		9.47
	-12.00	383.0		16.10
	-16.00	497.0		20.90
	-20.00	585.0		24.60
	-24.25	710.0		29.90

TABLE III

NAVION TAIL WIND TUNNEL TEST

Run II: Elevator Hinge Moment Coefficients at Constant Angle of Attack with Wire at .07c of Horizontal Tail

Date: 13 April 1958

1	2	3	4	5
α	δ_e	force	q	C_h
deg.	deg.	grams	psf	.000421 (col. 3)
0	0	20.0	24.122	- .84
	1.9	60.2		- 2.54
	3.7	99.0		- 4.17
	8.5	220.0		- 9.26
	12.4	320.0		-13.48
	16.0	427.0		-17.90
	19.8	546.0		-23.00
	- 8.4	225.0		+ 9.48
	- 4.0	55.1		2.32
	- 8.0	148.5		6.25
	-12.0	276.0		11.61
	-15.8	382.0		16.10
	-20.0	489.0		20.60
	-24.0	618.0		26.00
	- 4.2	77.0		3.24
	+ 8.5	198.0		- 8.34
	16.0	416.0		-17.50

TABLE IV

NAVION TAIL WIND TUNNEL TEST

Run III: Elevator Hinge Moment Coefficients at Constant Elevator Deflection

Date: 13 April 1958

1	2	3	4	5
α deg.	δ_e deg.	force grams	q psf	C_h .000421 (col. 3)
0	0	12.4	24.122	.0052
+ 2		32.6		.0137
4		52.2		.0220
6		70.8		.0290
8		92.3		.0389
10		122.2		.0515
- 2		4.9		.0021
- 4		12.4		.0052
- 2		4.1		.0017
0		21.6		.0091
+ 2		38.2		.0161
4		54.1		.0228
6		72.0		.0304
8		92.4		.0380
10		121.8		.0510
4		54.0		.0228
2		39.4		.0166
0		21.4		.0090
- 2		6.8		.0028
- 4		9.0		.0038

TABLE V

NAVION TAIL WIND TUNNEL TEST

Run IV: Elevator Hinge Moment Coefficients at Constant Elevator Deflection with Wire at .07c

Date: 13 April 1958

1	2	3	4	5
δ_e	α	force	q	C_h
deg.	deg.	grams	psf	.000421(col. 3)
0	0	--	24.122	--
	2	27.0		.0114
	4	39.4		.0166
	6	87.8*		.0370
	8	175.9*		.0741
	10	265.0*		.1116

*Buffeting Tail

TABLE VI

NAVION TAIL WIND TUNNEL TEST

Run V: Elevator Hinge Moment Coefficients at Constant Elevator Deflection with Wire at .07c

Date: 13 April 1958

1	2	3	4	5
δ_e	α	force	q	C_h
deg.	deg.	grams	psf	.000549 (col. 3)
0	0	11.9	18.512	.0065
	-2	3.6		.0020
	-4	4.5		.0025
	+2	19.8		.0109
	+4	29.2		.0159

TABLE VII

NAVION TAIL WIND TUNNEL TEST

Run VI: Elevator Hinge Moment Coefficients at Constant Elevator Deflection with Wire at .25c

Date: 13 April 1958

1	2	3	4	5
δ_e deg.	deg.	force grams	q psf	C_h .000549 (col. 3)
0	8	110.0*	18.512	.0604
	6	60.7		.0333
	4	36.0		.0198
	2	24.1		.0132
	0	13.3		.0073
	-2	3.6		.0020
	-4	6.8		.0037

* Buffeting Tail

TABLE VIII

NAVION TAIL WIND TUNNEL TEST

Run VII: Rudder Hinge Moment Coefficients at Constant Yaw

Date: 12 April 1958

1	2	3	4	5
ψ	δ_r	force	q	C_h
deg.	deg.	grams	psf	.000764 (col. 3)
0	0	3.75	24.122	.0029
	- 2	17.00		.0130
	- 4	34.00		.0260
	- 6	58.00		.0443
	- 8	79.00		.0603
	-10	112.50		.0859
	-10	110.00		.0840
	-12	141.00		.1075
	-14	180.00		.1393
	- 8	79.50		.0606
	0	5.50		.0042
	- 2	18.00		.0137
	- 4	37.00		.0282
	- 6	59.00		.0443
	0	4.75		.0036
	+ 2	- 12.50		-.0096
	4	- 36.00		-.0275
	6	- 59.00		-.0450
	8	- 79.50		-.0606
	10	-106.30		-.0810
	12	-137.50		-.1051
	14	-167.50		-.1275
	15	-182.00		-.1390
	8	- 78.00		-.0595
	8	- 82.50		-.0630
	4	- 38.00		-.0290
	4	- 38.50		-.0294

TABLE IX

NAVION TAIL WIND TUNNEL TEST

Run VIII: Rudder Hinge Moment Coefficients at Constant Yaw

Date: 12 April 1958

1	2	3	4	5
ψ deg.	δ_r deg.	force grams	q psf	C_h .00764(col.3)
0	0	5.0	24.122	.0038
	- 2	22.0		.0168
	- 4	40.0		.0305
	- 6	72.0		.0550
	- 8	79.6		.0607
	-10	115.0		.0878
	-14	180.0		.1375
	- 6	60.0		.0458
	- 4	38.0		.0290
	0	4.0		.0031
	+ 2	-15.2		-.0116
	4	-39.2		-.0299
	6	-59.0		-.0450
	8	-80.0		-.0610
	10	-105.0		-.0802
	12	-136.0		-.1040
	14	-168.0		-.1282

TABLE X

NAVION TAIL WIND TUNNEL TEST

Run IX: Rudder Hinge Moment Coefficients at Constant Yaw with Wire at .25c on Rudder Fin and Elevator

Date: 13 April 1958

1	2	3	4	5
ψ	δ_r	force	q	C_h
deg.	deg.	grams	psf	.000995 (col. 3)
0	0	- 4.5	18.512	-.0045
	- 2	+ 6.8		+.0068
	- 4	20.4		.0203
	- 6	32.9		.0327
	- 8	45.4		.0450
	-10	60.2		.0616
	-12	77.1		.0767
	-14	95.4		.0948
	- 8	46.5		.0462
	+ 2	- 15.9		-.0158
	4	- 29.5		-.0294
	6	- 44.2		-.0440
	8	- 63.5		-.0631
	10	- 81.6		-.0811
	12	-100.0		-.0995
	14	-124.8		-.1232
	8	- 65.8	18.675	-.0650

TABLE XI

NAVION TAIL WIND TUNNEL TEST

Run X: Rudder Hinge Moment Coefficients at Constant Yaw with No Rudder Trim Tab and with Wire at .25c of Rudder and Elevator

Date: 13 April 1958

1	2	3	4	5
ψ	δ_r	force	q	C_h
deg.	deg.	grams	psf	.00102(col. 3)
0	0	- 6.8	18.512	-.0069
	- 2	+ 4.5		+.0046
	- 4	15.9		.0162
	- 6	29.1		.0296
	- 8	40.8		.0416
	-10	56.3		.0573
	-12	70.4		.0716
	-14	87.4		.0890
	- 8	43.2		.0440
	2	- 15.4		-.0157
	4	- 29.5		-.0300
	6	- 44.2		-.0450
	8	- 59.0		-.0600
	10	- 77.2		-.0786
	12	- 96.5		-.0984
	14	-118.0		-.1200

TABLE XII

NAVION TAIL WIND TUNNEL TEST

Run XI: Rudder Hinge Moment Coefficients at Constant Yaw with a Smooth Trim Tab

Date: 13 April 1958

1	2	3	4	5
ψ	δ_r	force	q	C_h
deg.	deg.	grams	psf	.000955 (col. 3)
0	0	1.8	18.512	.0018
	- 2	4.8		.0048
	- 4	27.2		.0270
	- 6	39.8		.0396
	- 8	55.6		.0553
	-10	71.5		.0711
	-12	88.5		.0880
	-14	113.5		.1128
	-14	113.5		.1128
	- 2	17.1		.0170
	0	1.8		.0018
	2	- 7.9		-.1079
	4	- 25.0		-.0248
	6	- 43.2		-.0430
	8	- 60.0		-.0596
	10	- 84.0		-.0835
	12	-109.0		-.1085
	14	-136.5		-.1351
	6	- 43.6		-.0433

TABLE XIII

NAVION TAIL WIND TUNNEL TEST

Run XII: Rudder Hinge Moment Coefficients at Constant Rudder Deflection

Date: 12 April 1958

1	2	3	4	5
ψ deg.	δ_r deg.	force grams	q psf	C_h .0184/q (col. 3)
0	0	2.0	24.122	.0015
- 2.0		0		0
- 4.0		- 10.3		.0079
- 6.0		- 18.2		.0139
- 8.0		- 26.3		.0207
-10.0		- 51.3		.0391
-12.0		- 67.8		.0517
-13.0		- 77.0		.0587
0		+ 1.0		.0008
+ 2.0		7.0		.0053
4.0		17.0		.0130
6.0		30.0		.0229
8.1		49.6		.0378
10.0		62.5		.0477
12.5		100.0		.0763

TABLE XIV

NAVION TAIL WIND TUNNEL TEST

Run XIII: Rudder Hinge Moment Coefficients at Constant Rudder Deflection

Date: 12 April 1958

1	2	3	4	5
ψ	δ_r	force	q	C_h
deg.	deg.	grams	psf	.0184/q (col. 3)
0	0	- 2.0	24.122	.0015
- 2.0		- 5.0		.0038
- 4.0		- 16.0		.0122
- 6.0		- 27.0		.0206
- 8.0		- 39.5		.0301
- 8.0		- 39.0	23.836	.0301
-14.2		-106.0		.0818
+ 2.0		+ 5.0		.0039
4.0		15.0		.0116
6.0		26.2	23.467	.0205
8.0		41.5		.0325
8.0		39.2		.0307
10.0		61.0		.0478
10.0		73.0		.0572
12.0		95.0	23.181	.0753
15.0		150.0	23.017	.1198

TABLE XV

NAVION TAIL WIND TUNNEL TEST

Run XIV: Rudder Hinge Moment Coefficients at Constant Rudder Deflection with a Smooth Tab

Date: 13 April 1958

1	2	3	4	5
ψ	δ_r	force	q	C_h
deg.	deg.	grams	psf	.0184/q (col. 3)
0	0	1.0	18.582	.0011
- 2		- 3.2		.0032
- 6		-15.9		.0157
-10		-38.6		.0382
-14		-73.7		.0729
0		+ 2.3		.0022
+ 2		9.1		.0090
6		25.0		.0247
10		43.2		.0428
14		88.0		.0871
6		25.0		.0247

TABLE XVI

NAVION TAIL WIND TUNNEL TEST

Run XV: Rudder Hinge Moment Coefficients at Constant Rudder Deflection with Wire at .25c of Rudder and Elevator

Date: 13 April 1958

1	2	3	4	5
ψ	δ_r	force	q	C_h
deg.	deg.	grams	psf	.0184/q (col. 3)
- 2	0	-11.4	18.582	.0112
- 4		-21.4		.0212
- 6		-33.6		.0333
- 8		-44.2		.0437
-10 *		-59.0		.0584
-12 *		-76.2		.0754
-14 *		-87.8		.0869
- 8		-44.2		.0437
+ 2		- 1.1		.0011
4		+ 7.9		.0079
6		19.3		.0191
8		28.6		.0283
10 *		40.8		.0404
12 *		51.7		.0512
14 *		73.8		.0731

*Buffeting Tail

TABLE XVII

NAVION TAIL WIND TUNNEL TEST

Run XVI: Rudder Hinge Moment Coefficients at Constant Rudder Deflection with No Rudder Trim Tab and Wire at .25c of Rudder and Elevator

Date: 13 April 1958

1	2	3	4	5
ψ	δ_r	force	q	C_h
deg.	deg.	grams	psf	.01886/q (col. 3)
0	0	- 6.8	18.582	.0069
- 2		-10.2		.0104
- 6		-21.6		.0219
-10		-48.8		.0496
-14		-75.0		.0761
+ 2		- 2.9		.0026
6		+17.1		.0173
10		38.6		.0392
14 *		65.9		.0670

* Buffeting Tail

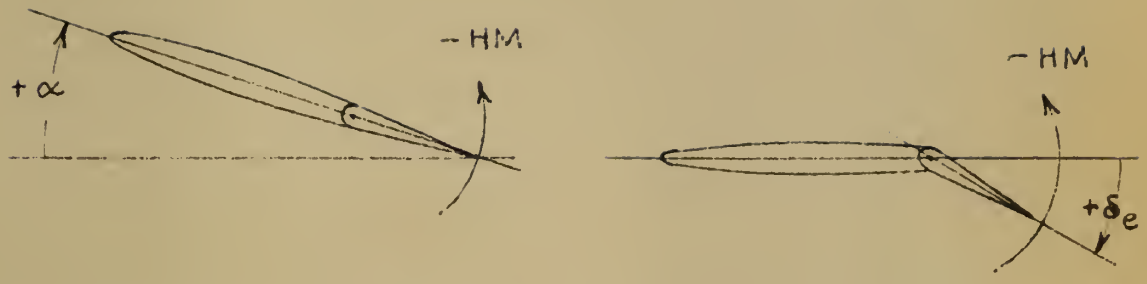

Elevator Convention

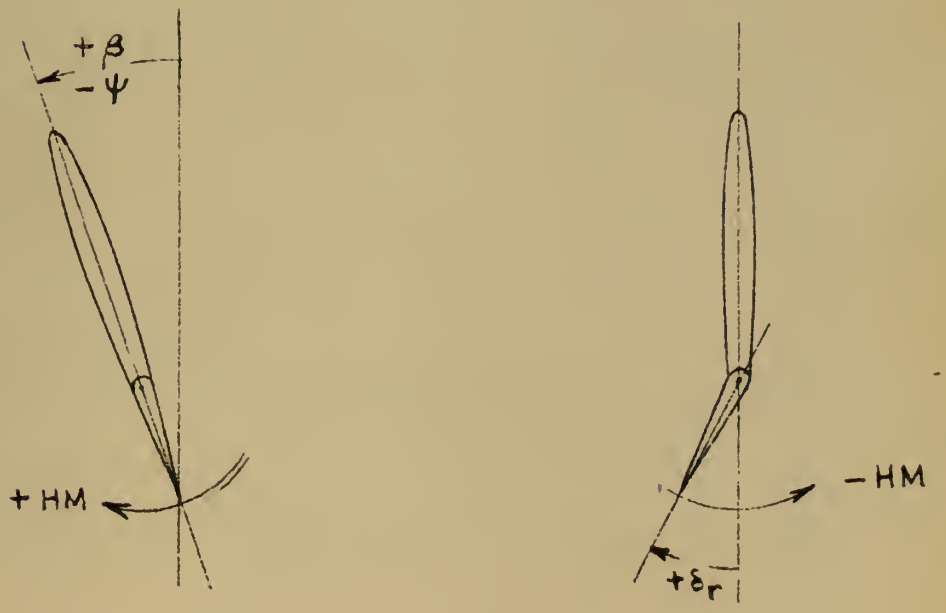

Rudder Convention

Fig. 1 Sign Conventions

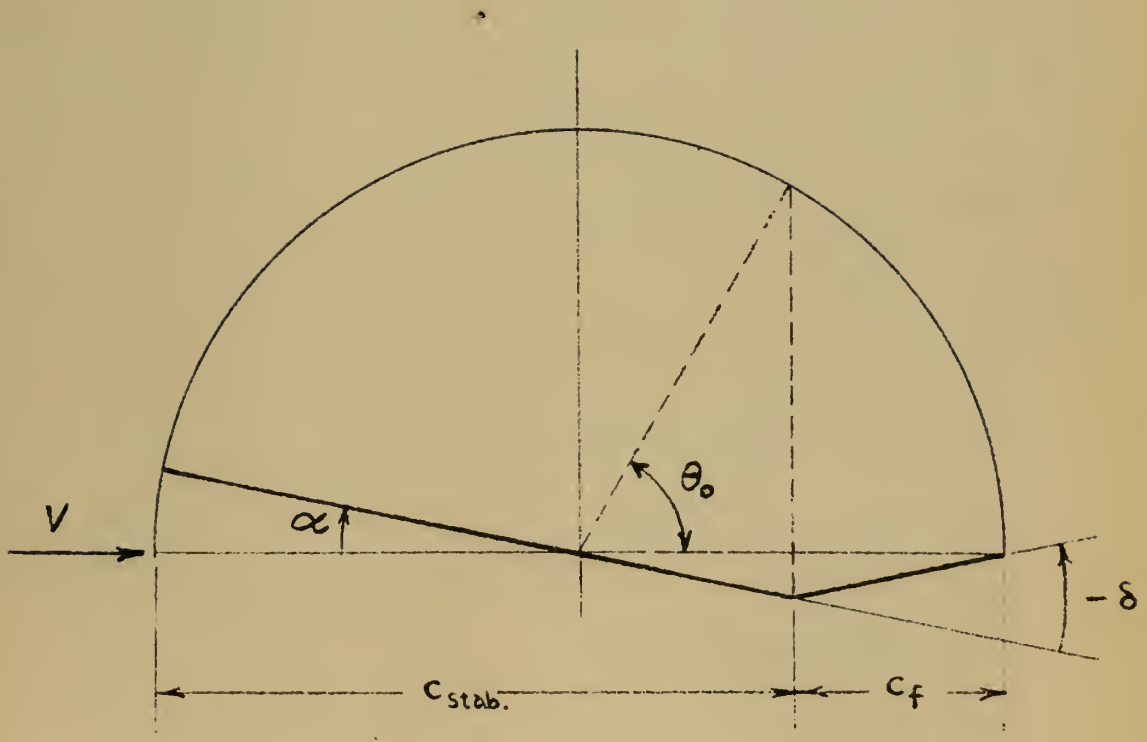

Fig. 2 Diagram Showing Determination of Angle θ_o used in Analytical Development (Thin Airfoil Theory)

Fig. 2

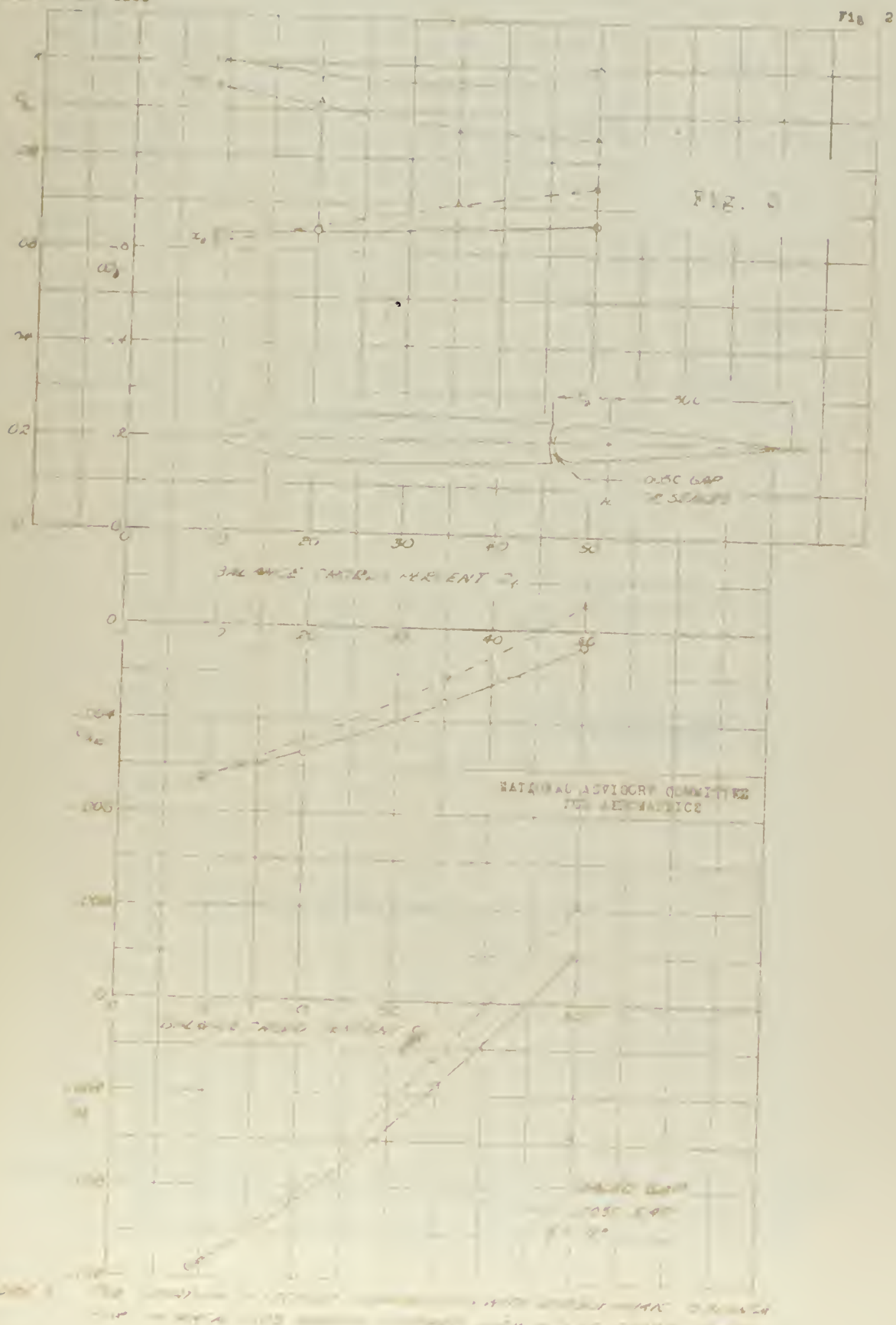

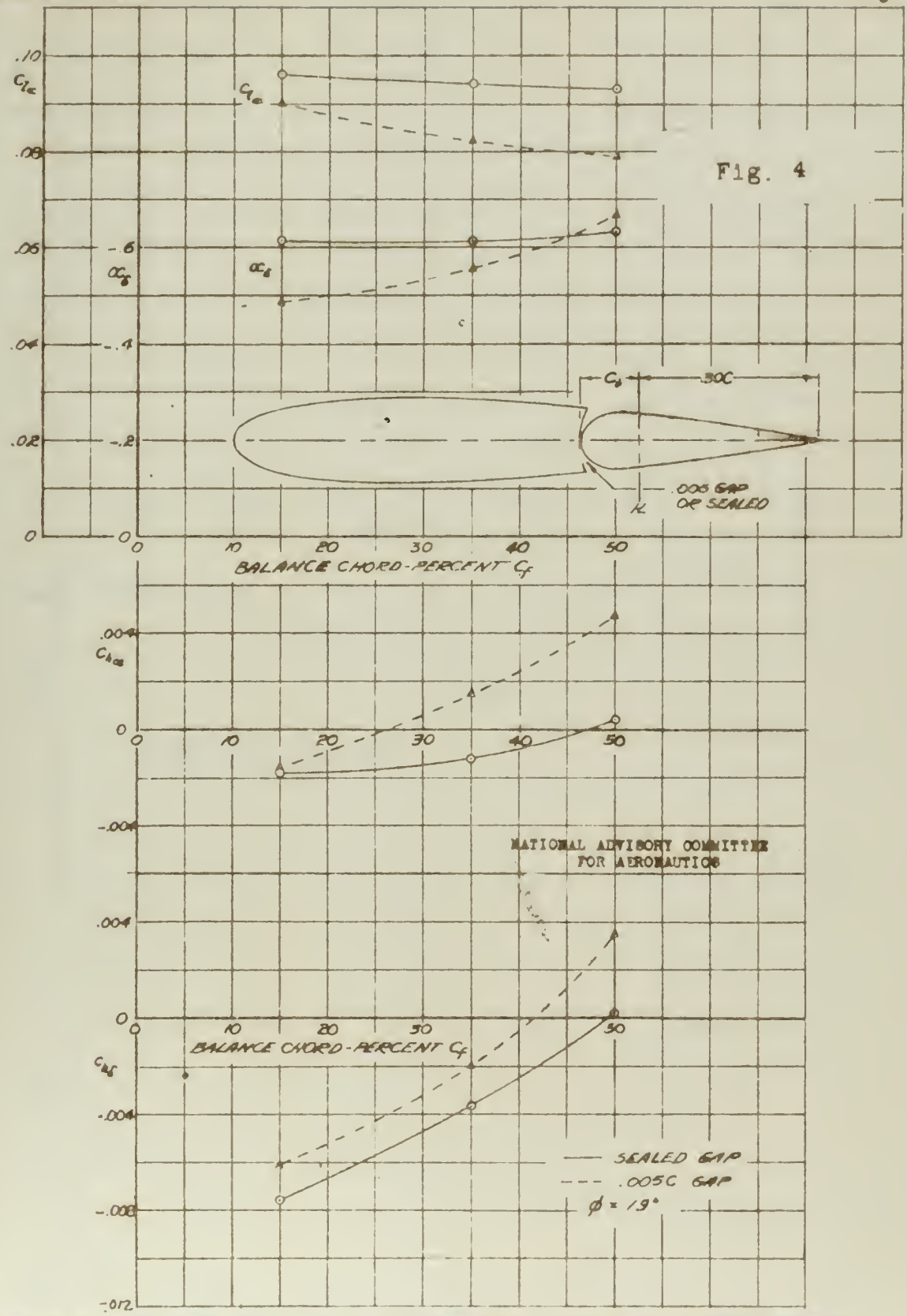

FIGURE 4.- THE VARIATION OF SECTION PARAMETERS WITH AERODYNAMIC BALANCE FOR AN NACA 0015 AIRFOIL EQUIPPED WITH A 0.30-CHORD FLAP WITH A BLUNT NOSE PROFILE. ADAPTED FROM REF. 6, 7, AND 8.

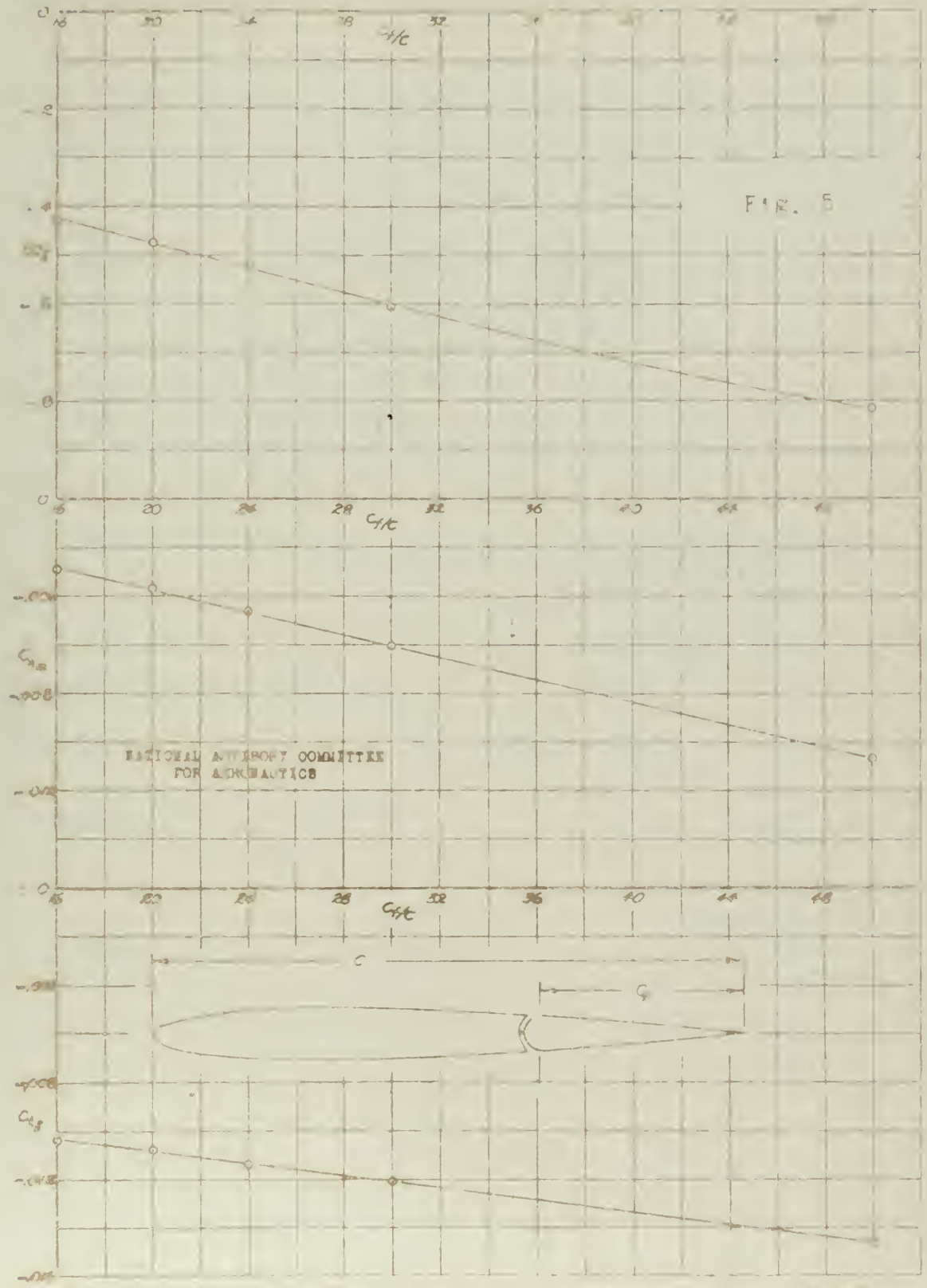

FIGURE 6.- THE VARIATION OF SECTION PARAMETERS WITH CONTROL-SURFACE CHORD FOR AN NACA 0009 AIRFOIL EQUIPPED WITH A PLAIN SEALED FLAP. FROM REFERENCE 1.

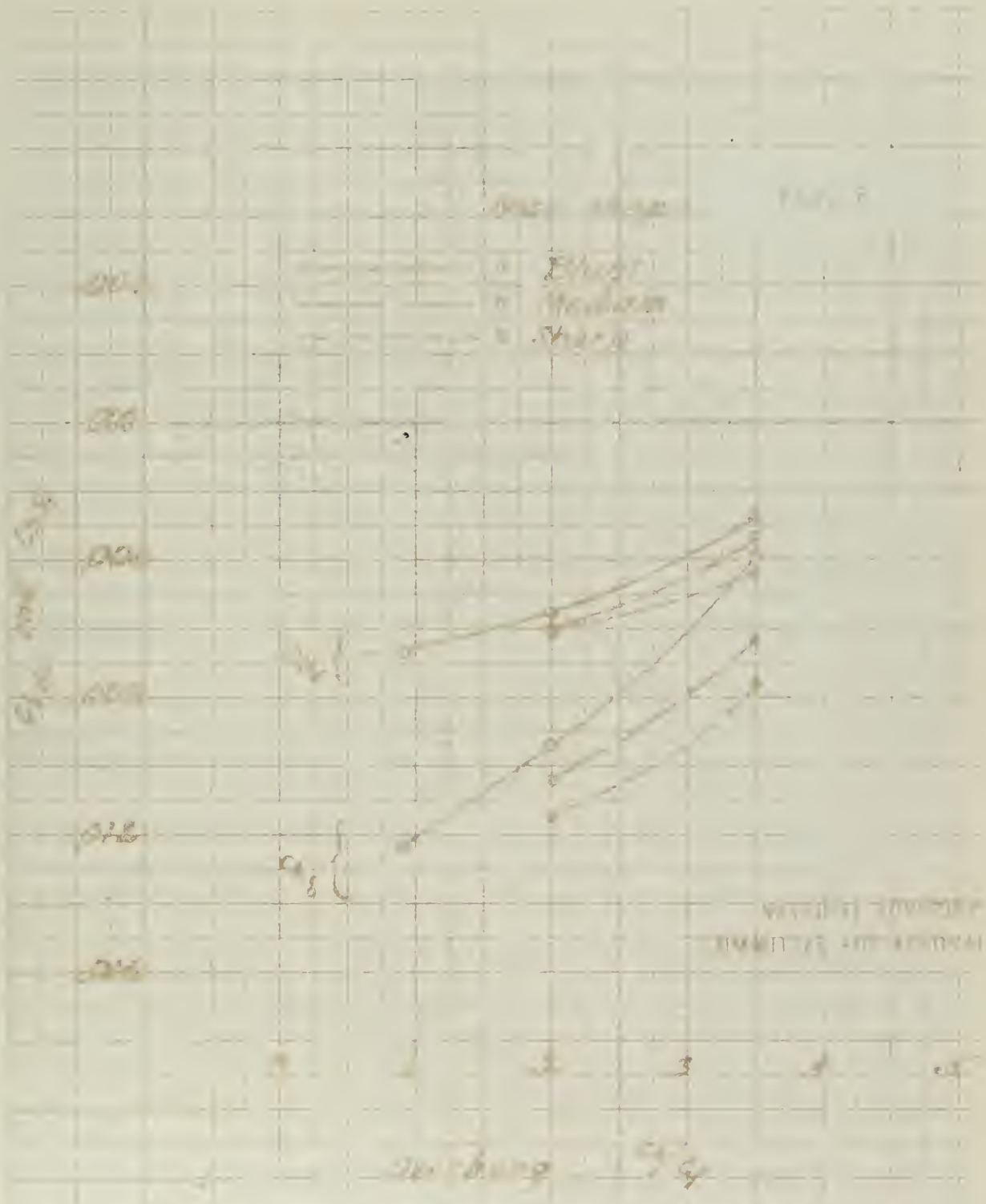

Figure 14.4 Continued

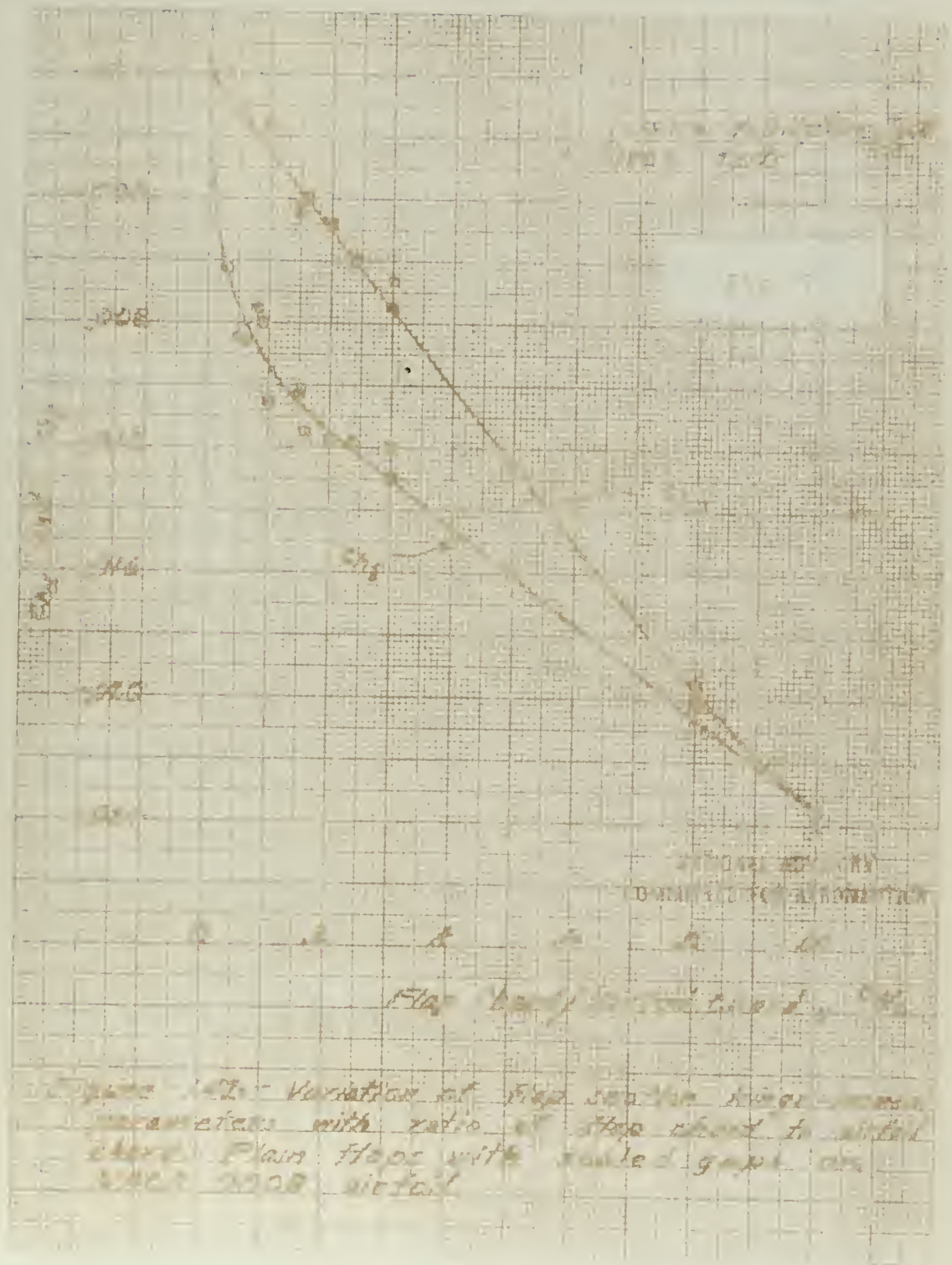

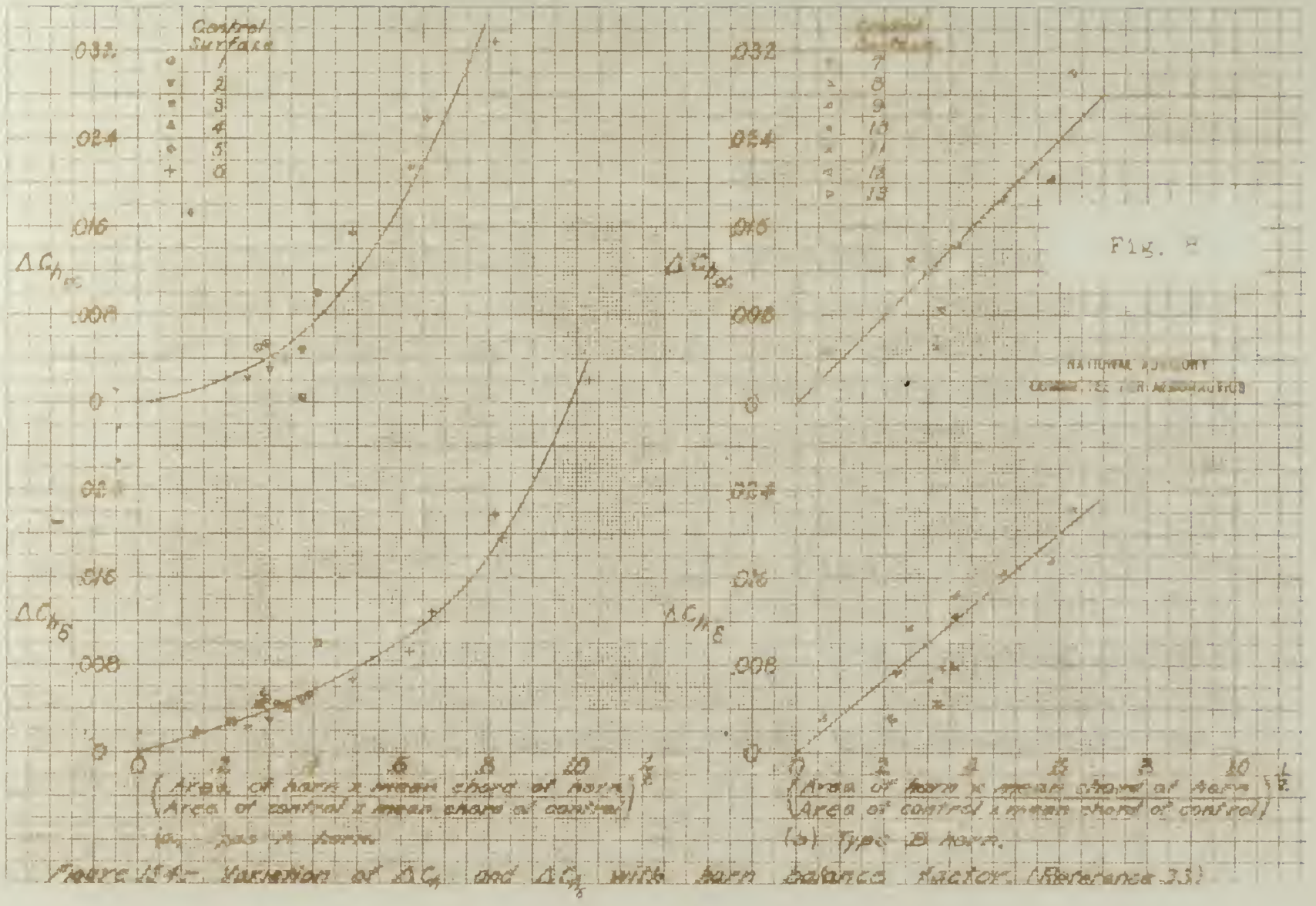

(a) Type A horn.

(b) Type B horn.

Figure 14.- Variation of $\Delta C_{h_{tc}}$ and ΔC_{h_δ} with horn balance factor. (Reference 33)

Fig. 14

SUBSONIC INSTRUCTIONAL WIND TUNNEL

Top View

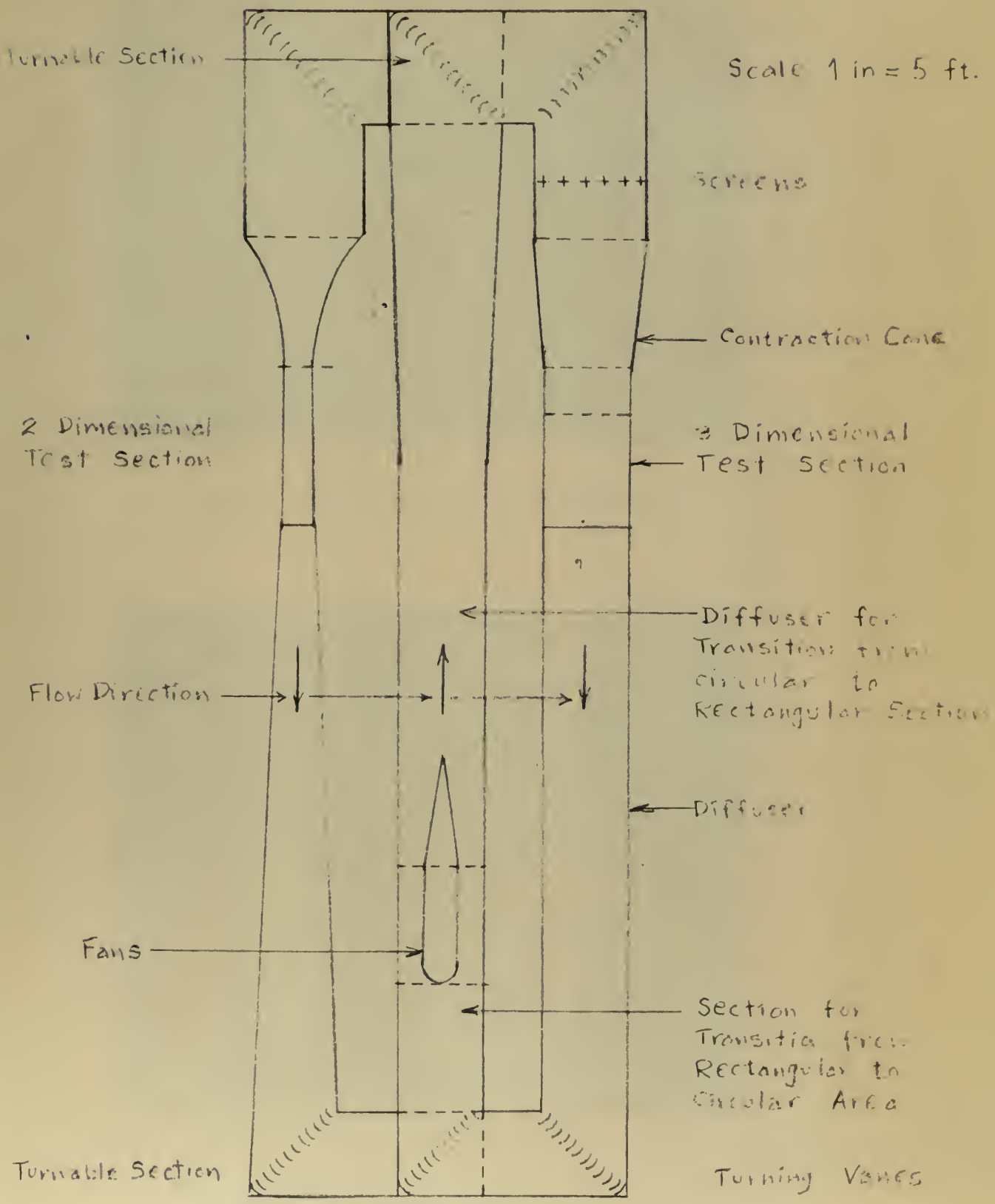

Fig. 9

Fig. 10 Model installed in test section

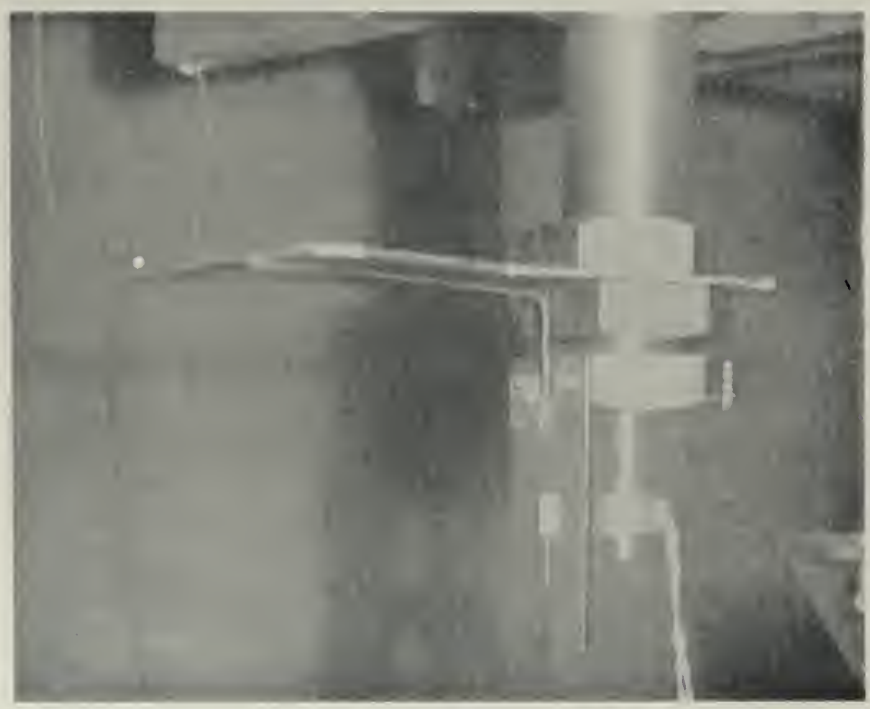

Fig. 11 View beneath test section showing rudder strain gage beam

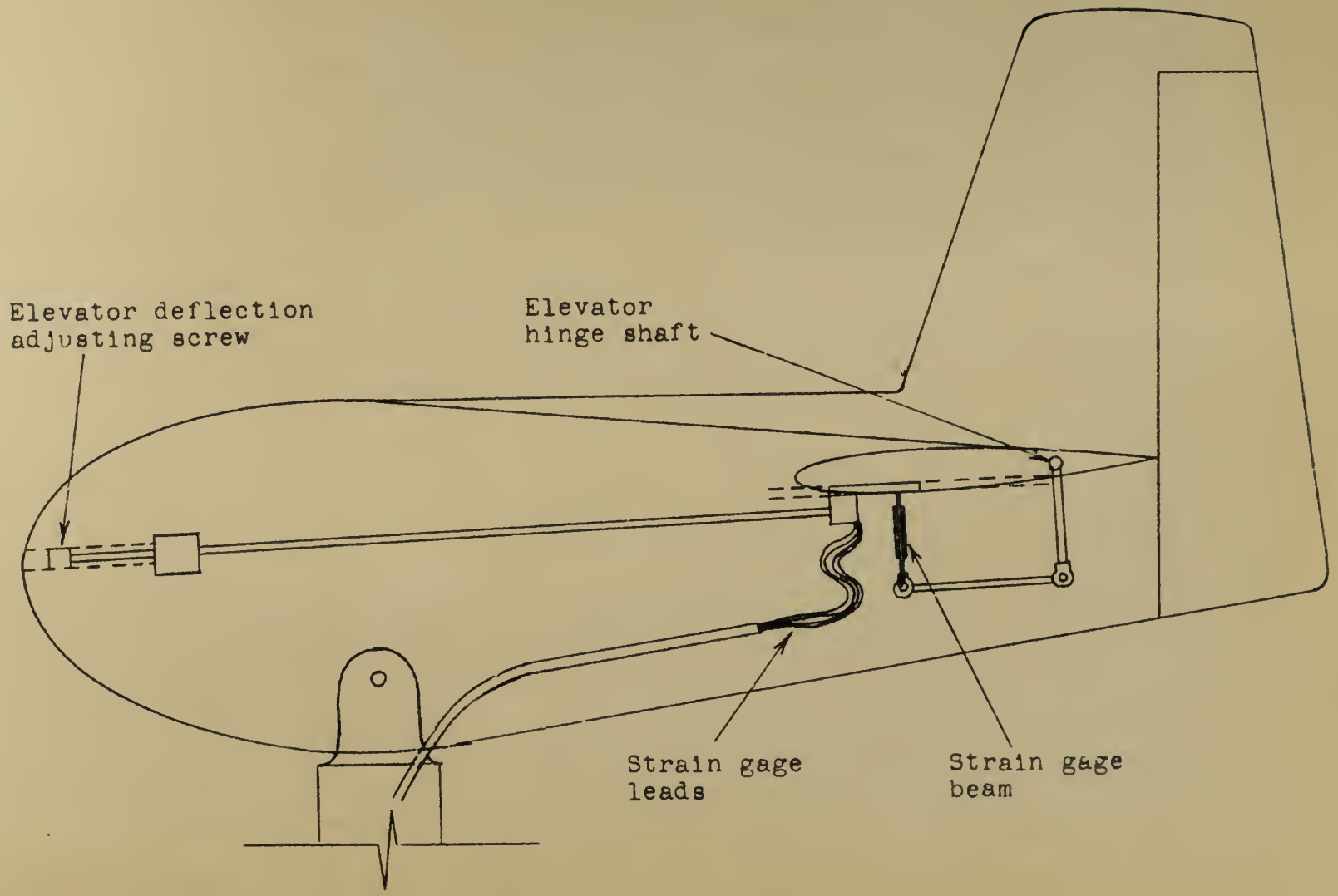

Fig. 12 Side view schematic of model

Fig. 13

Effect of Elevator Deflection on

Horizontal Tail Lift

$\frac{S_e}{S_t} = \frac{14.098}{43.061} = .3272$

From Fig. 5-33 $\tau = 0.53$

$d\alpha_t = \tau\, d\delta_e$

$= .53\, \delta_e$

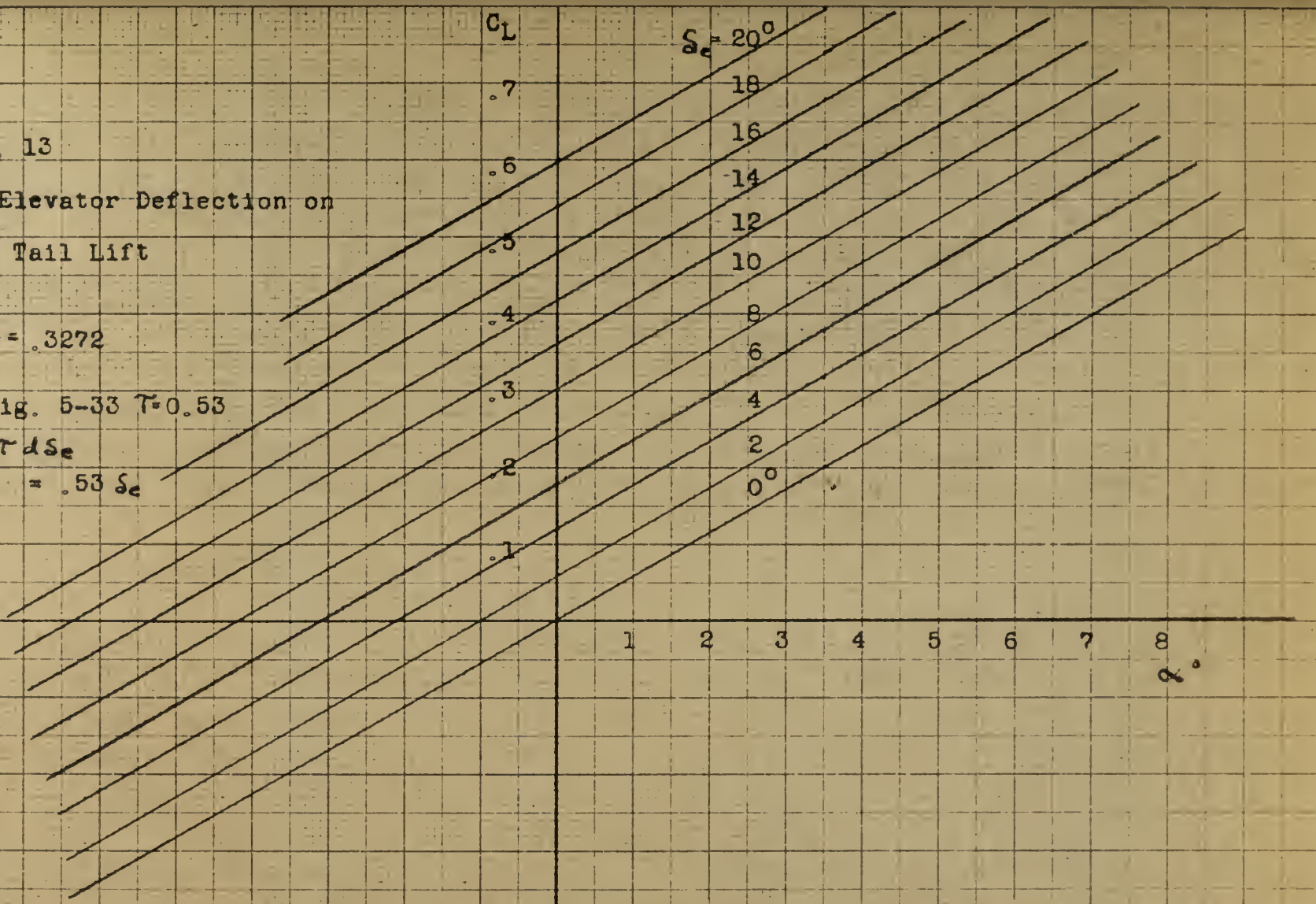

Fig. 14

Effect of Rudder Deflection on Vertical Tail Force

$\frac{S_r}{S_{V_t}} = \frac{6.052}{12.925} = .4679$

From Fig. 5-33 $\tau = 0.638$

$d\sigma = \tau_r d\delta_r$

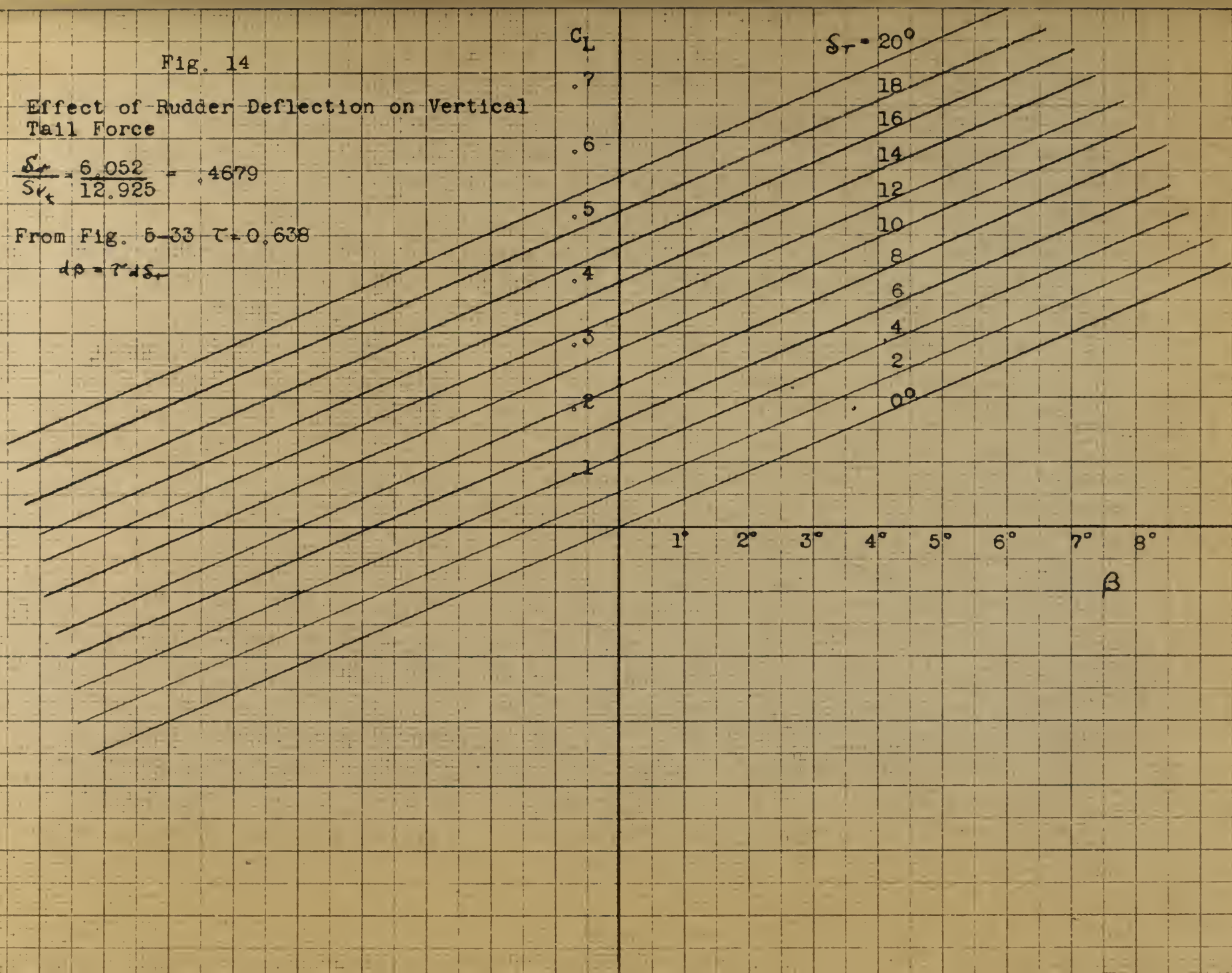

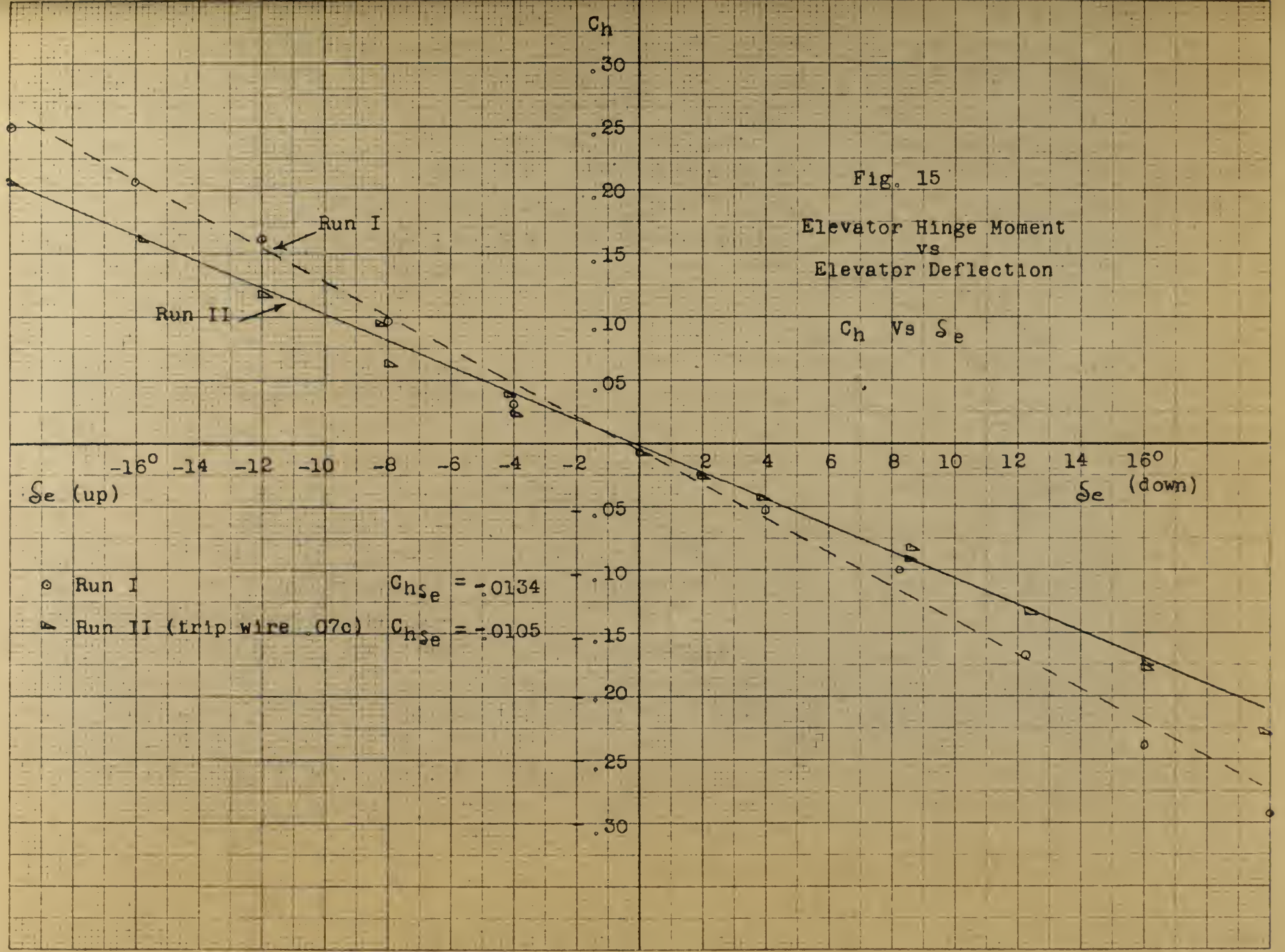

Fig. 15

Elevator Hinge Moment
vs
Elevator Deflection

C_h Vs δ_e

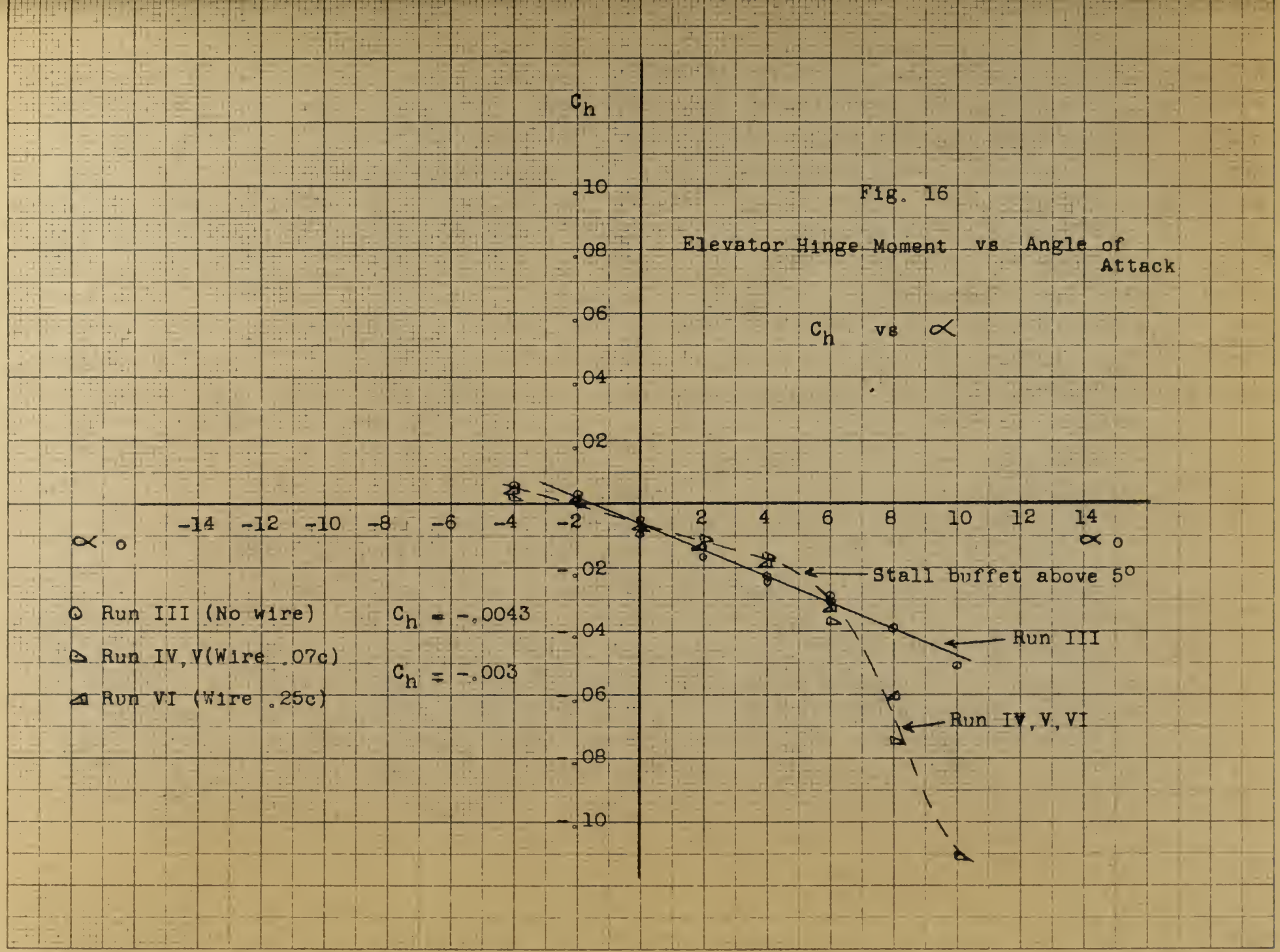
C_h
.10
.08
.06
.04
.02
-.02
-.04
-.06
-.08
-.10
-14 -12 -10 -8 -6 -4 -2 2 4 6 8 10 12 14
α o
α o
Fig. 16
Elevator Hinge Moment vs Angle of Attack
C_h vs α
Stall buffet above 5°
Run III
Run IV, V, VI
Run III (No wire)
Run IV, V (Wire .07c)
Run VI (Wire .25c)
C_h = -.0043
C_h = -.003

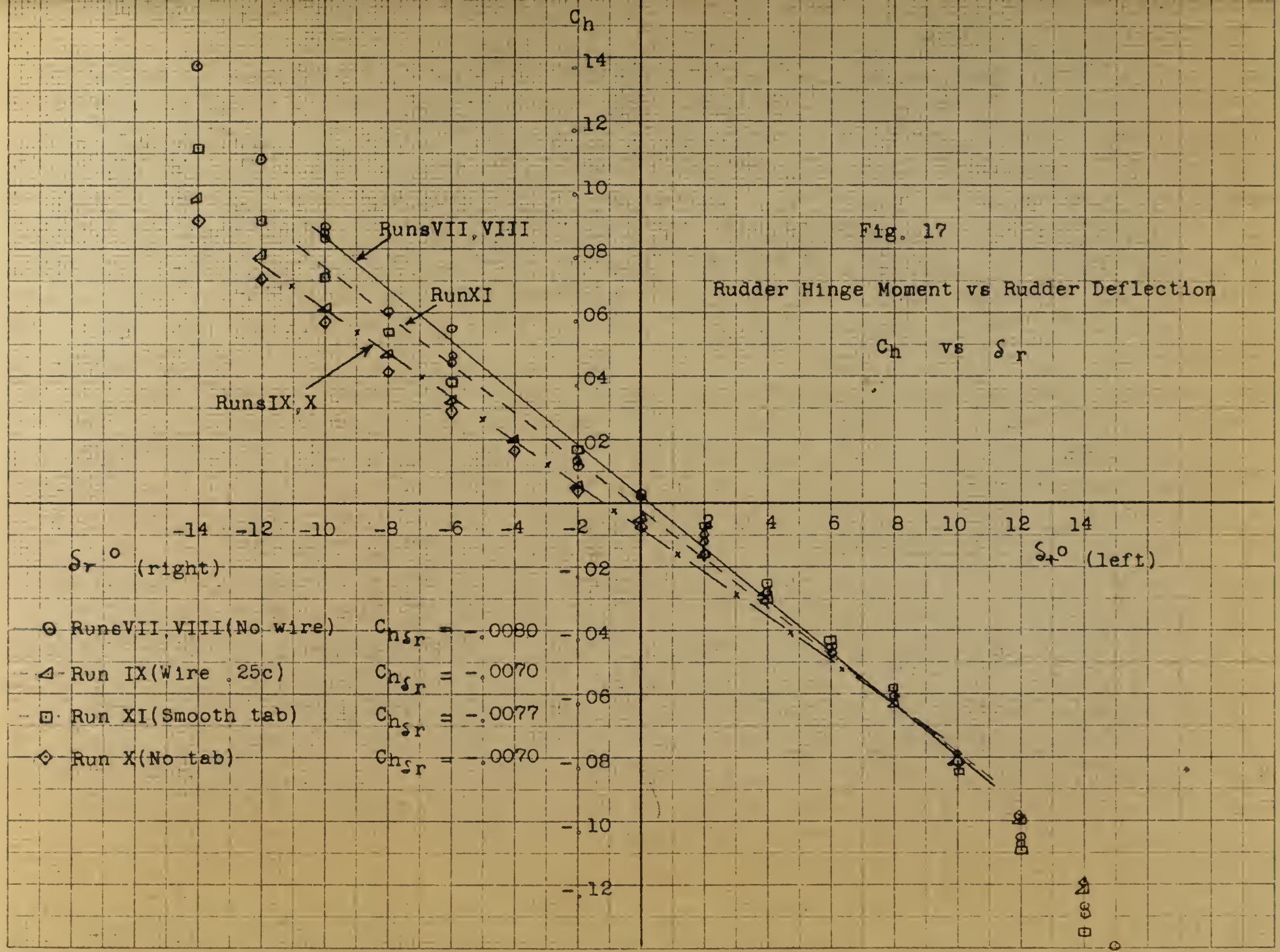

Fig. 17

Rudder Hinge Moment vs Rudder Deflection

C_h vs δ_r

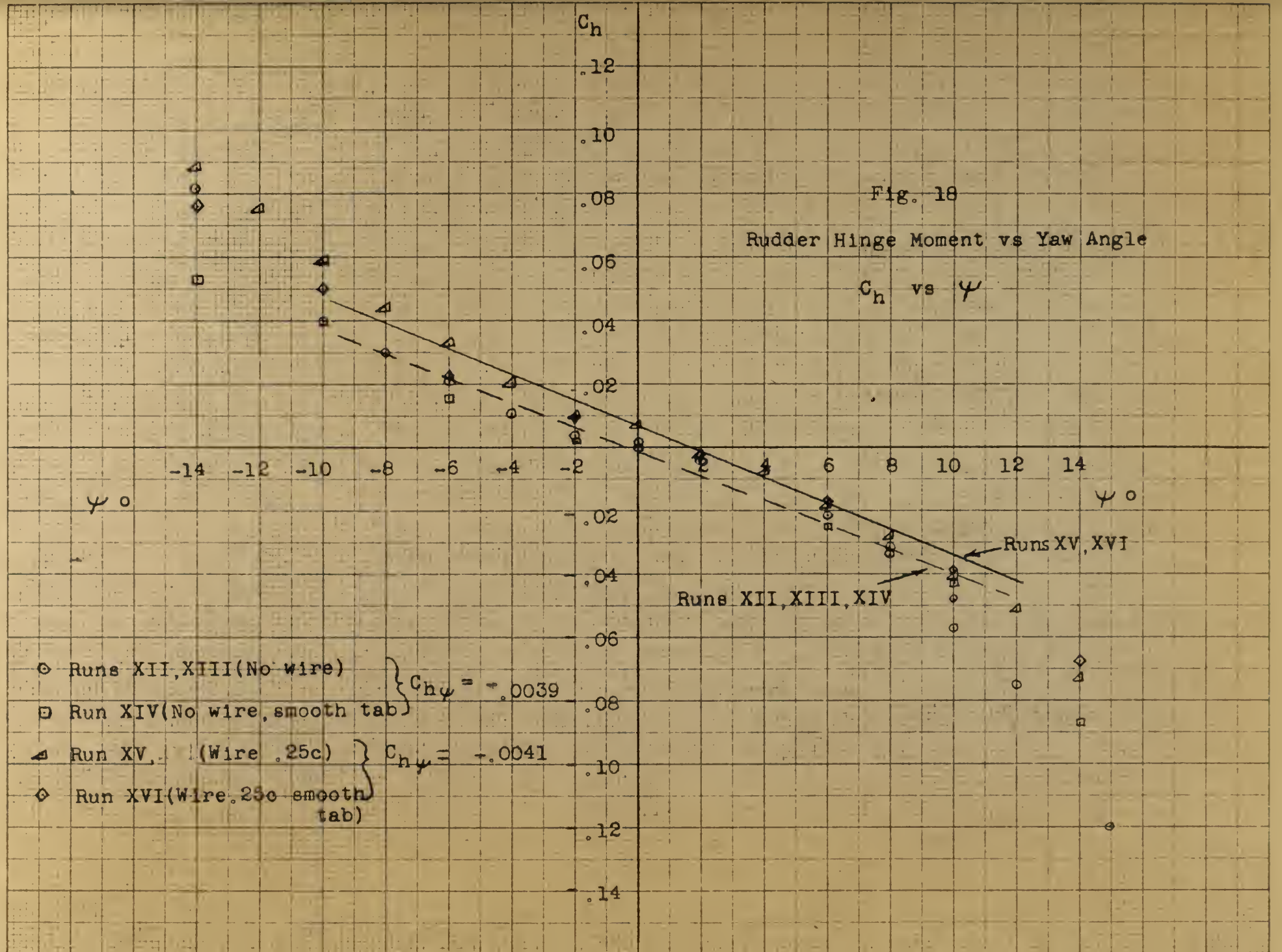

Fig. 18

Rudder Hinge Moment vs Yaw Angle

C_h vs ψ

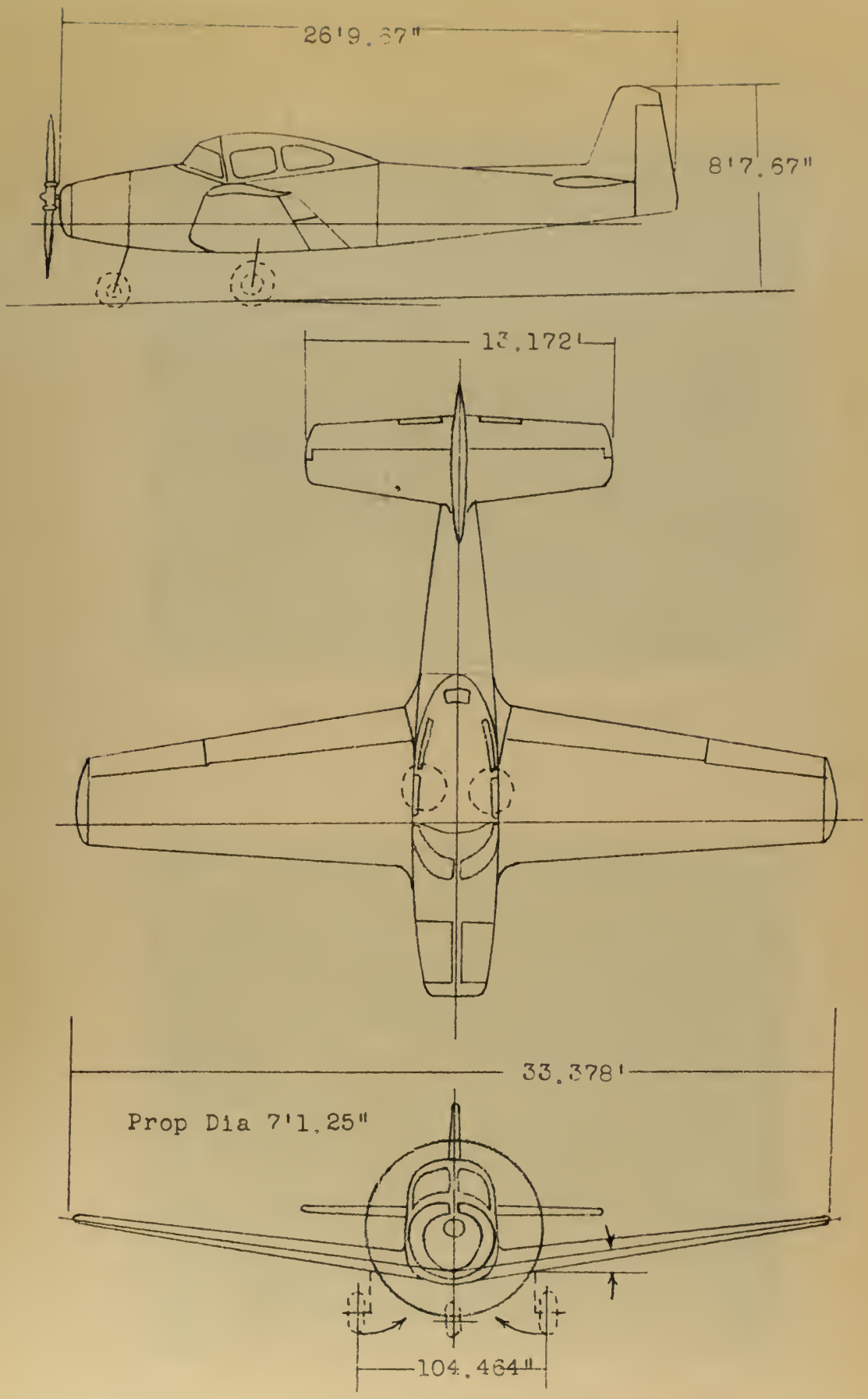

Fig.19 General Three-view drawing

Fig. 20 Test aircraft, Navion N91566

Fig. 21 Strain gage instrumented wheel for measuring stick force

Fig. 22 Strain gage instrumented beam for measuring rudder pedal force

Fig. 23 Rudder pedal strain gage beam installed in aircraft

Fig. 24 Elevator deflection indicating potentiometer

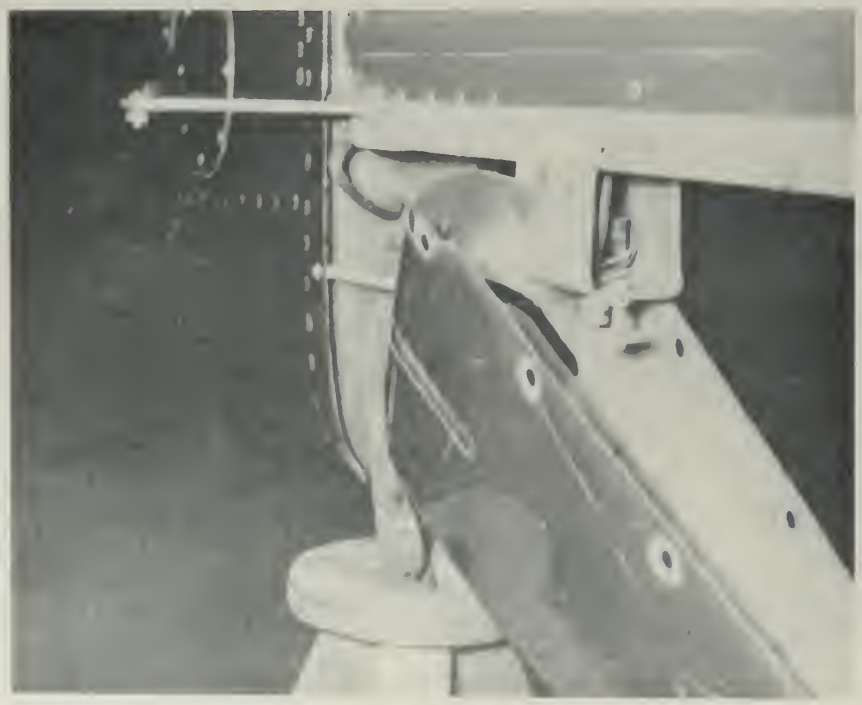

Fig. 25 Rudder deflection indicating potentiometer

Fig. 26 Side slip chute

Fig. 27 Side slip angle indicating vane

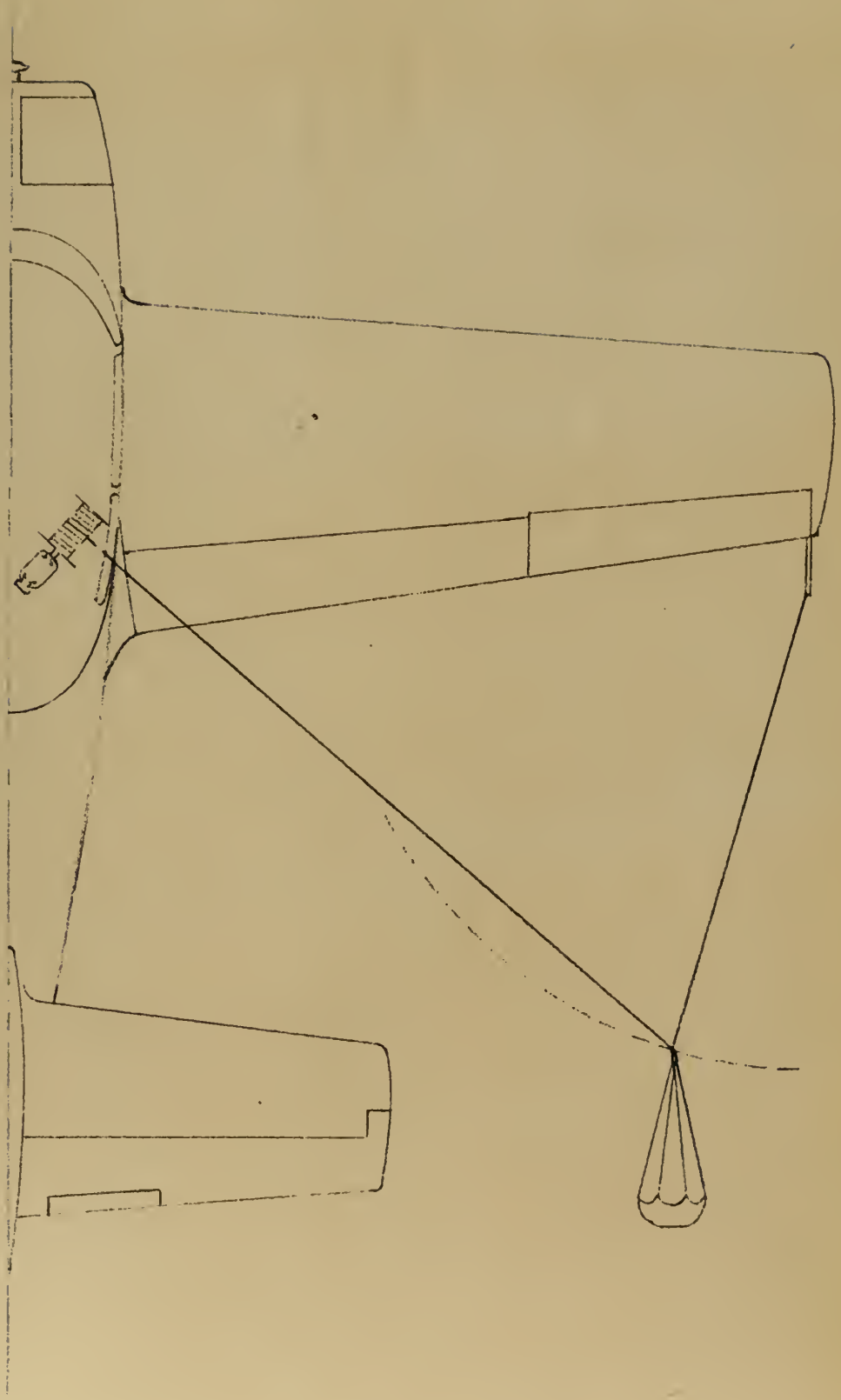

Fig. 28 Drawing of sideslip chute installation

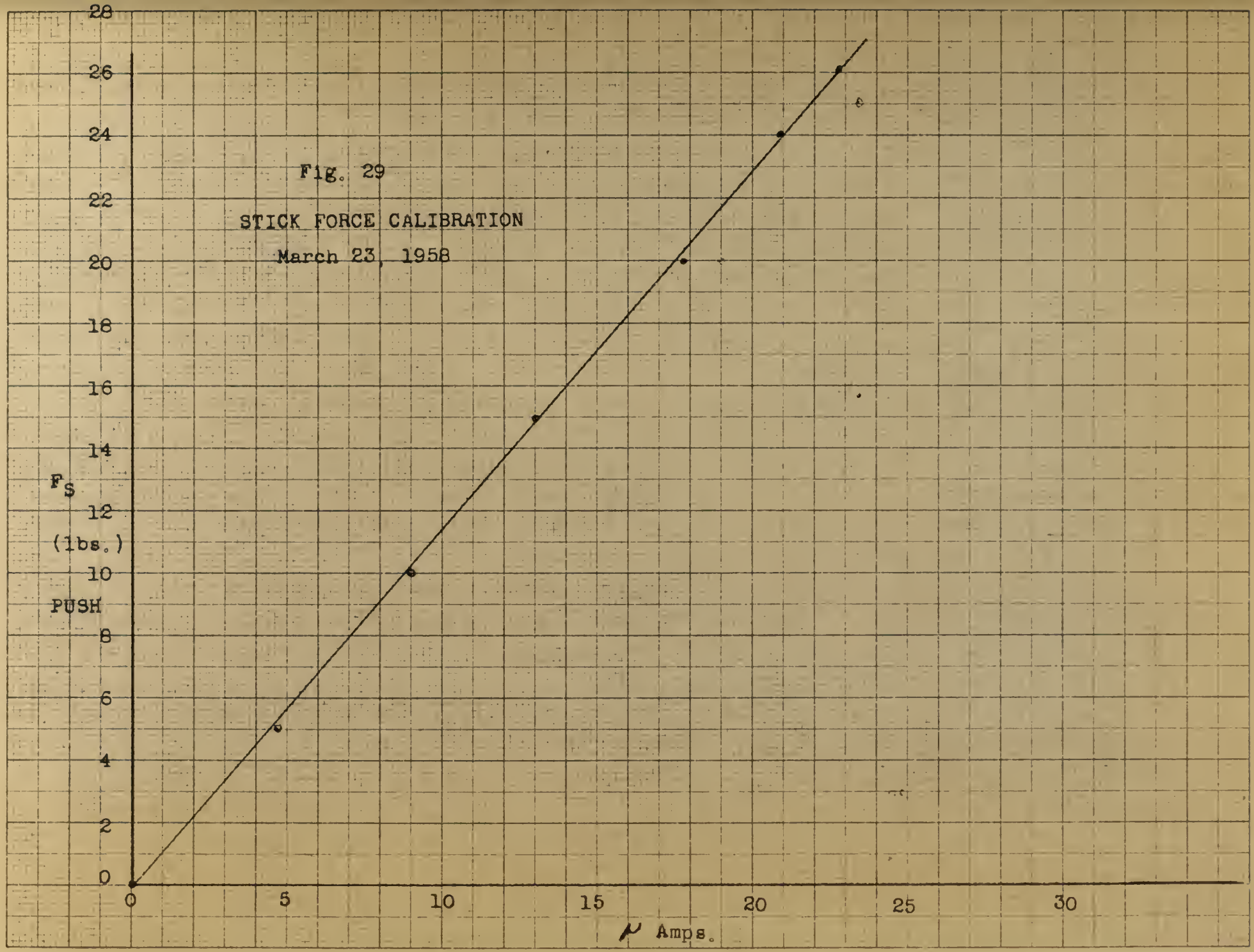
Fig. 29
STICK FORCE CALIBRATION
March 23, 1958
F_S
(lbs.)
PUSH
28
26
24
22
20
18
16
14
12
10
8
6
4
2
0
0
5
10
15
20
25
30
μ Amps.

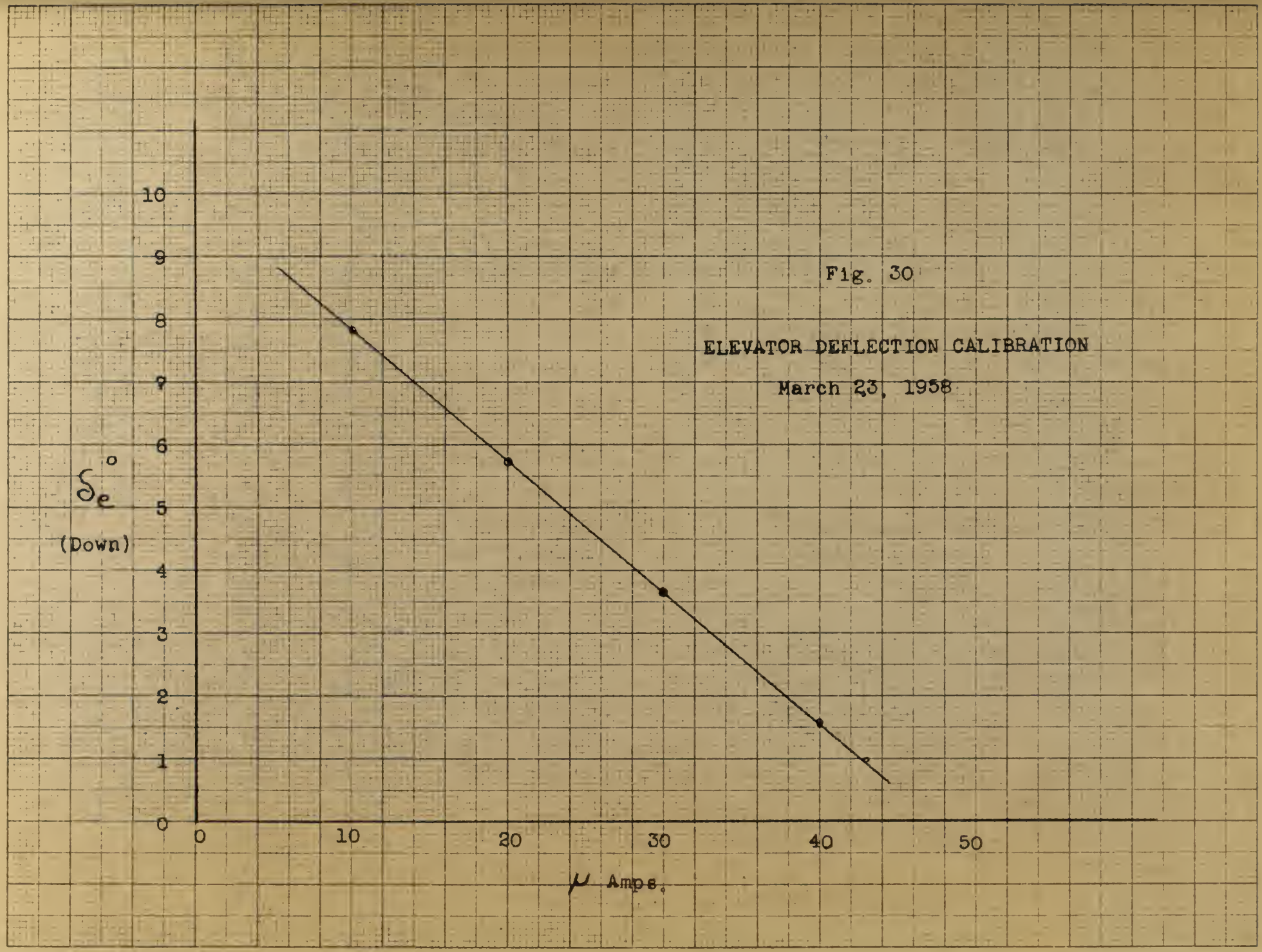
Fig. 30
ELEVATOR DEFLECTION CALIBRATION
March 23, 1956
δ_e °
(Down)
10
9
8
7
6
5
4
3
2
1
0
0
10
20
30
40
50
μ Amps.

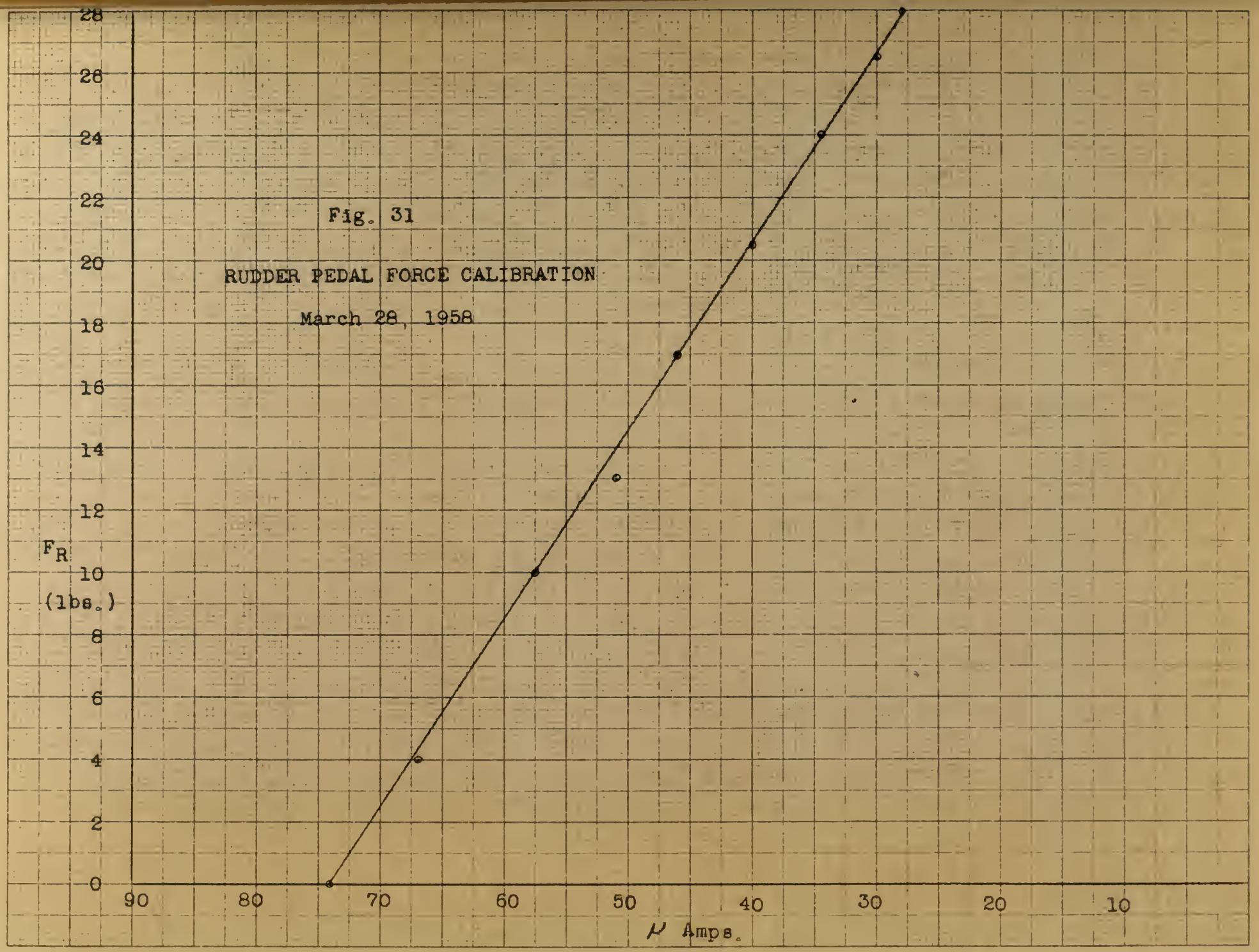
Fig. 31
RUDDER PEDAL FORCE CALIBRATION
March 28, 1958
F_R (lbs.)
28
26
24
22
20
18
16
14
12
10
8
6
4
2
0
90
80
70
60
50
40
30
20
10
μ Amps.

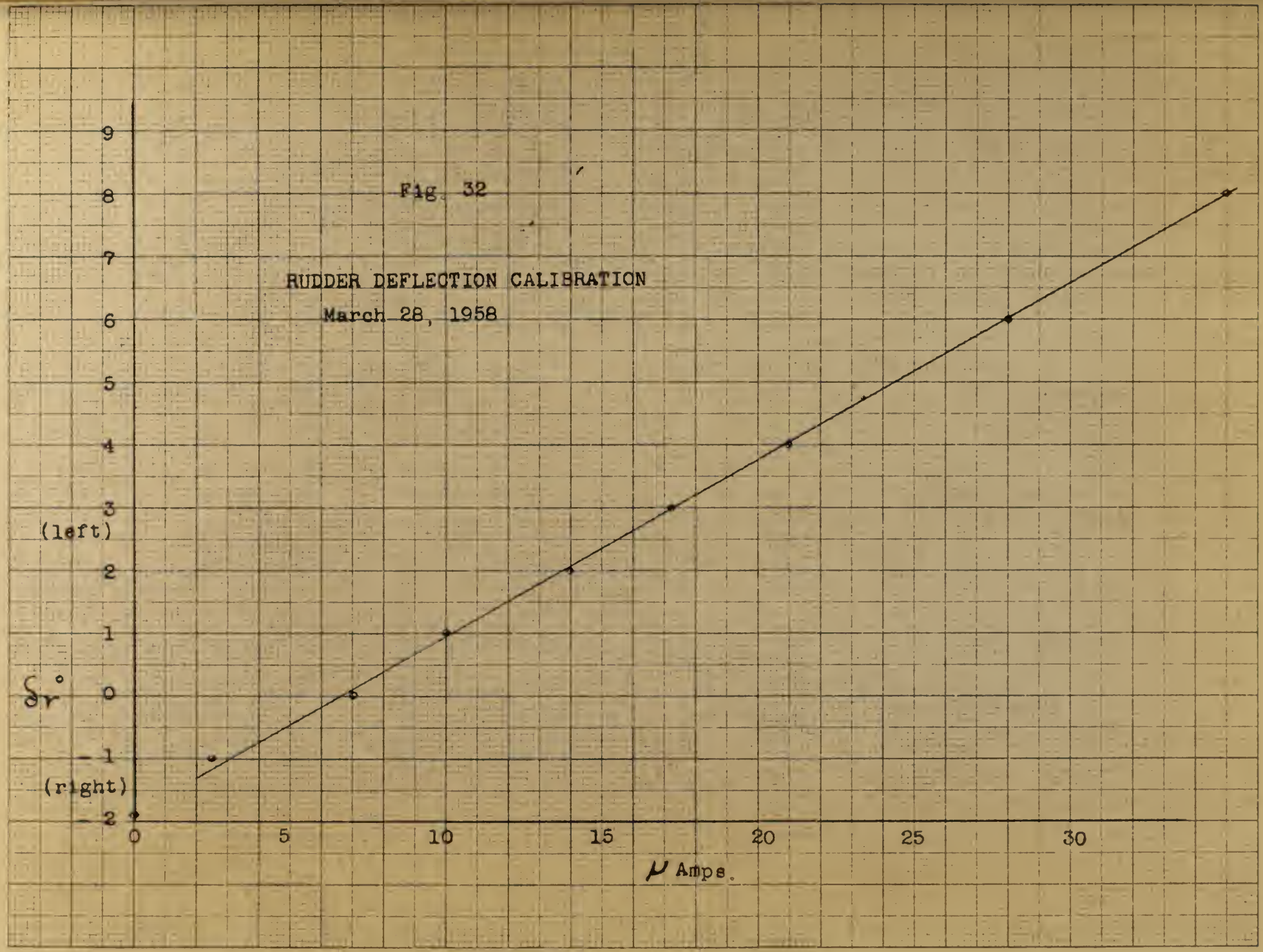
Fig. 32
RUDDER DEFLECTION CALIBRATION
March 28, 1958
9
8
7
6
5
4
3
(left)
2
1
δ_r°
0
-1
(right)
-2
0
5
10
15
20
25
30
μ Amps.

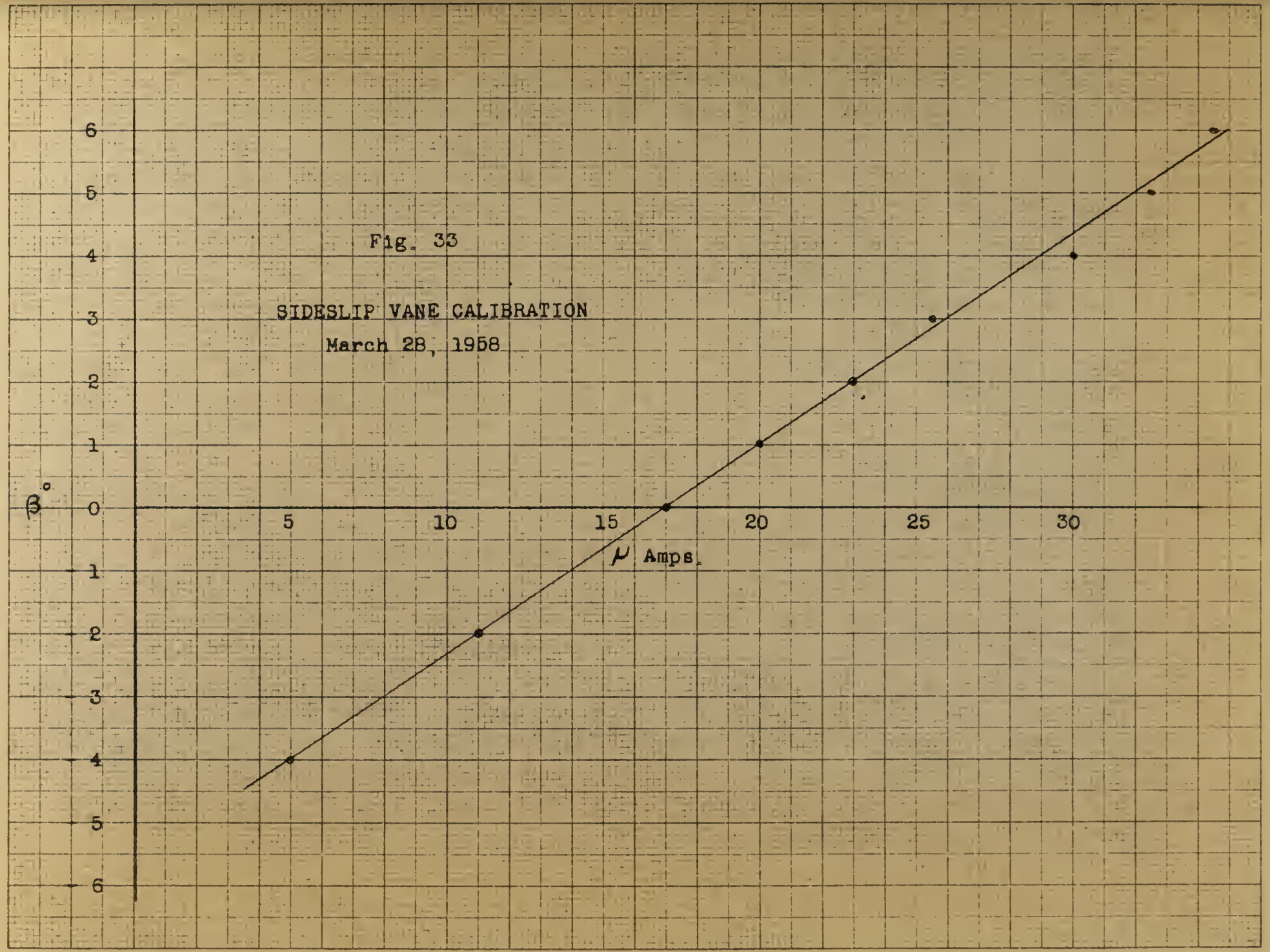
Fig. 33
SIDESLIP VANE CALIBRATION
March 28, 1958
β°
6
5
4
3
2
1
0
1
2
3
4
5
6
5
10
15
20
25
30
μ Amps.

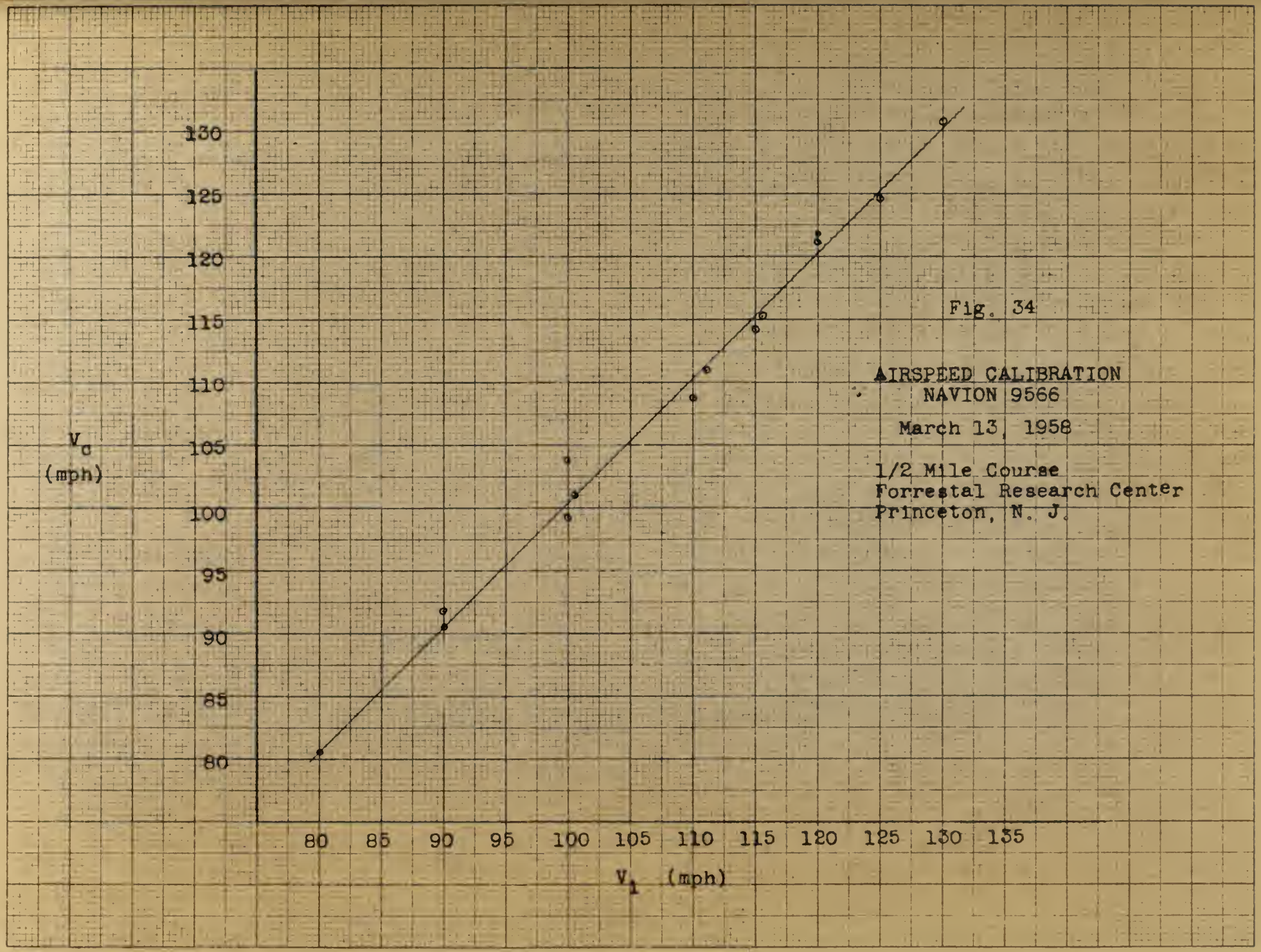

Fig. 34

AIRSPEED CALIBRATION
NAVION 9566

March 13, 1958

1/2 Mile Course
Forrestal Research Center
Princeton, N. J.

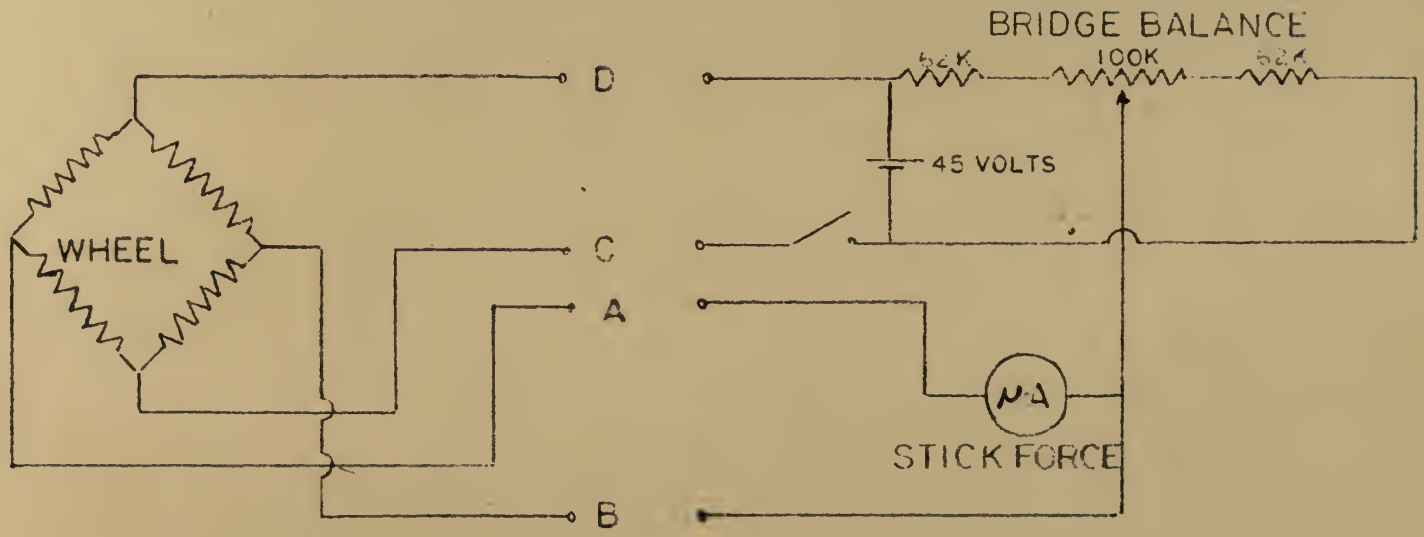

ELEVATOR STICK FORCE CIRCUIT

Fig. 35

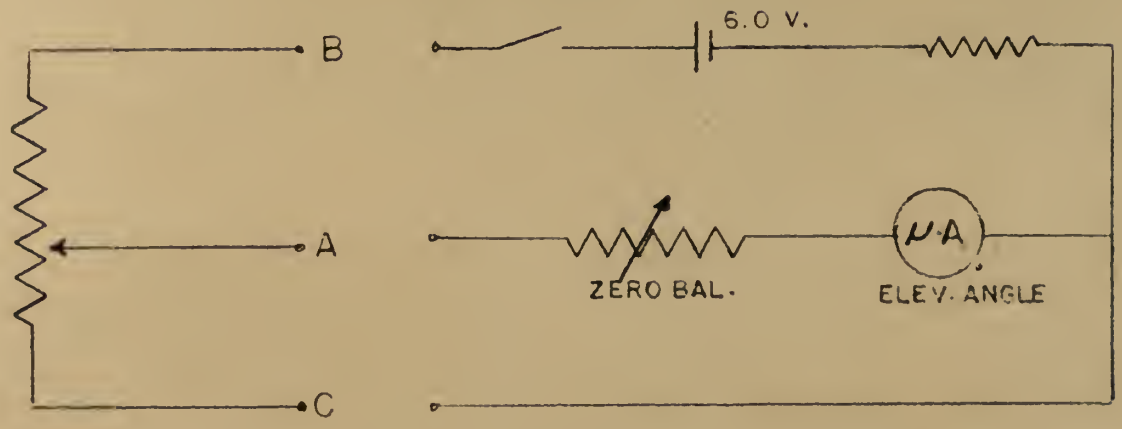

ELEVATOR DEFLECTION CIRCUIT

Fig. 36

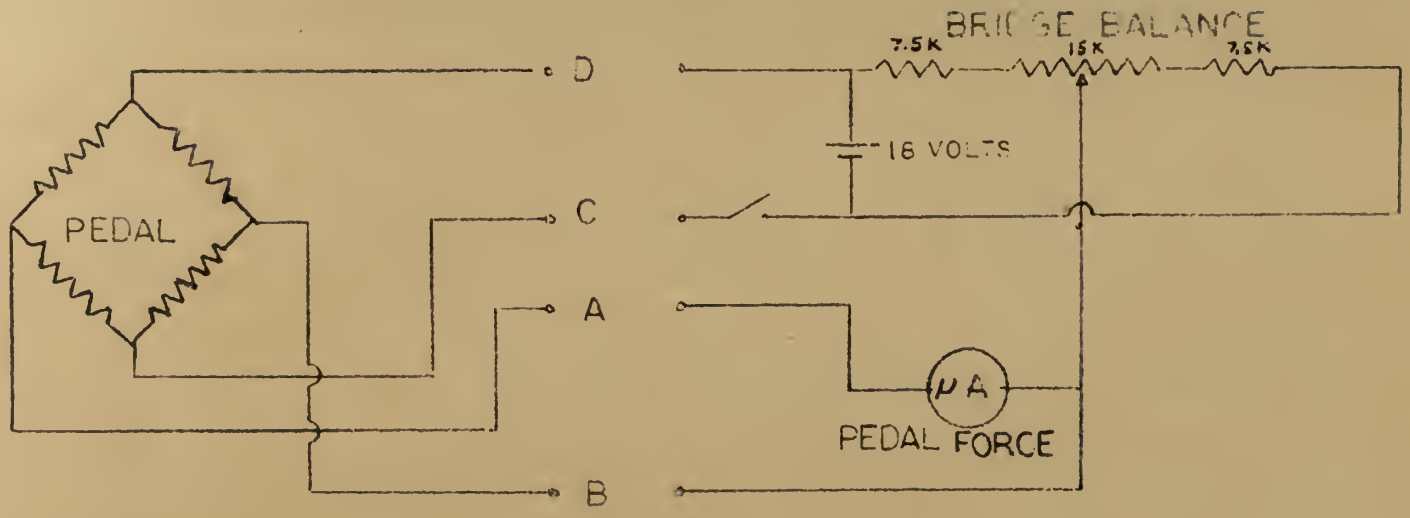

RUDDER PEDAL FORCE CIRCUIT

Fig. 37

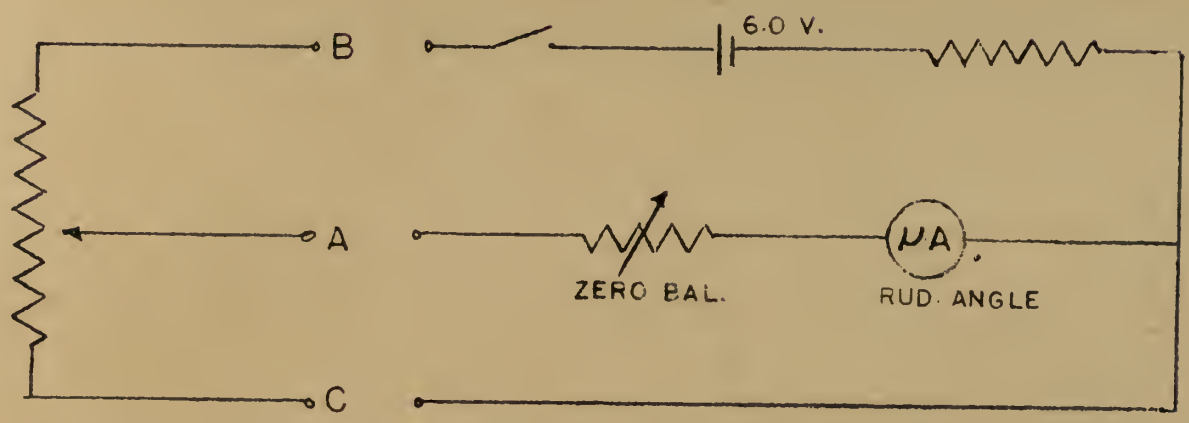

RUDDER DEFLECTION CIRCUIT

Fig. 38

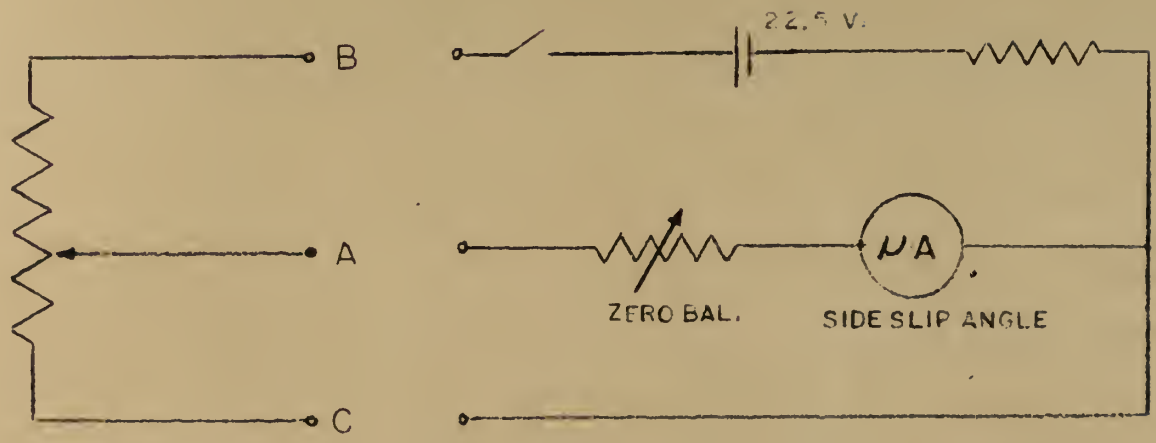

SIDE SLIP VANE DEFLECTION CIRCUIT

Fig. 39

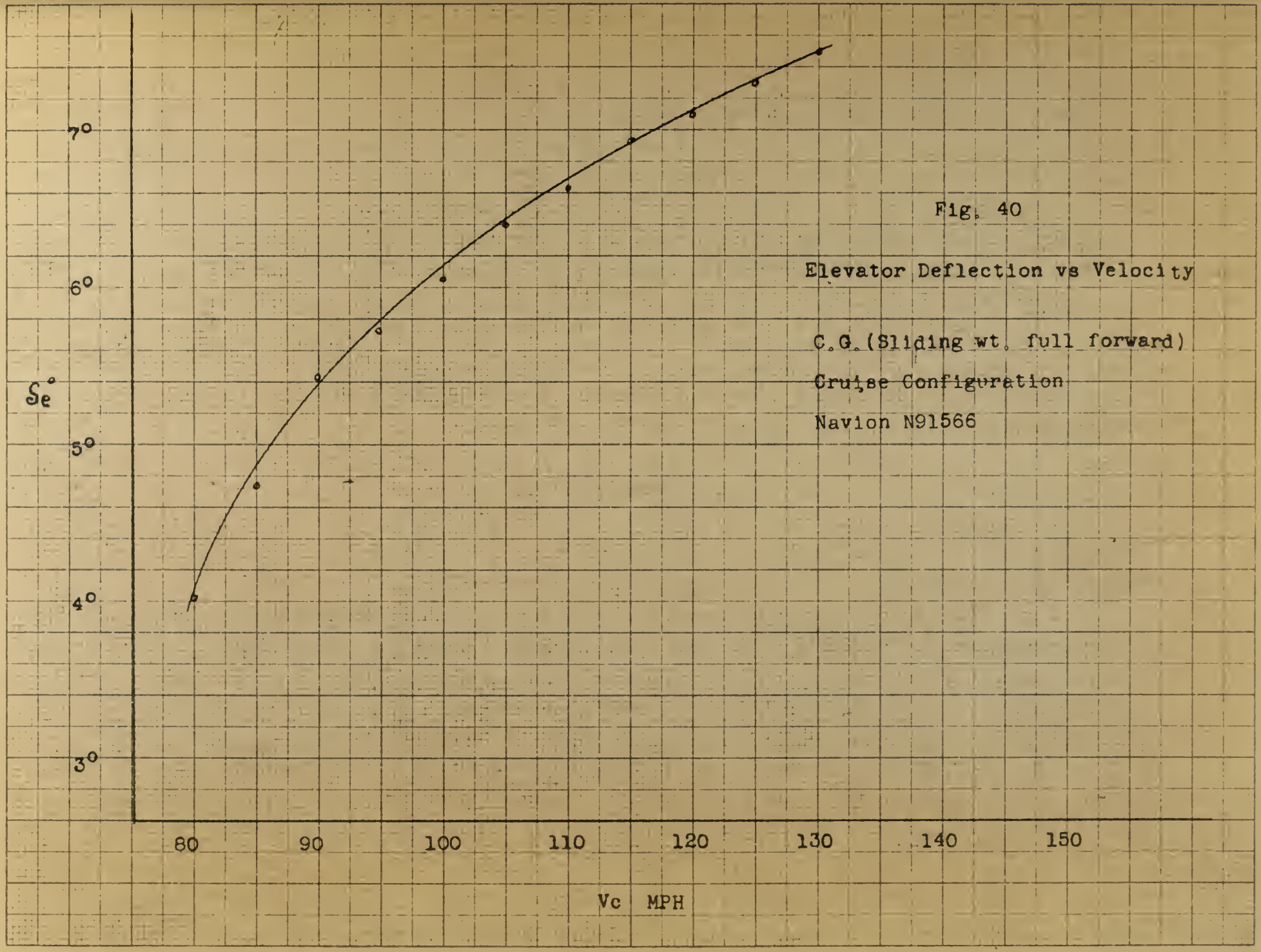

Fig. 40

Elevator Deflection vs Velocity

C.G. (Sliding wt. full forward)

Cruise Configuration

Navion N91566

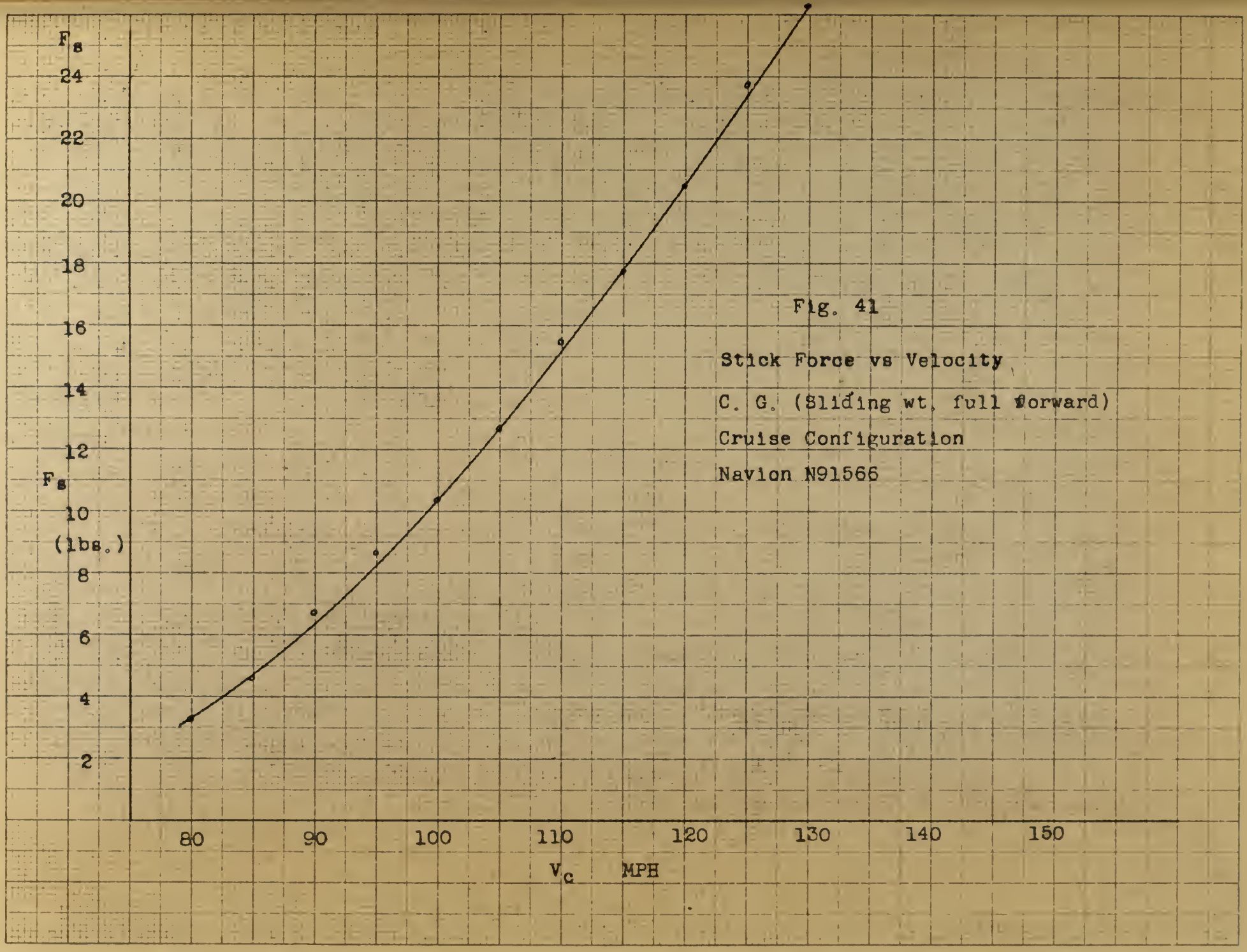

Fig. 41

Stick Force vs Velocity

C. G. (Sliding wt. full forward)

Cruise Configuration

Navion N91566

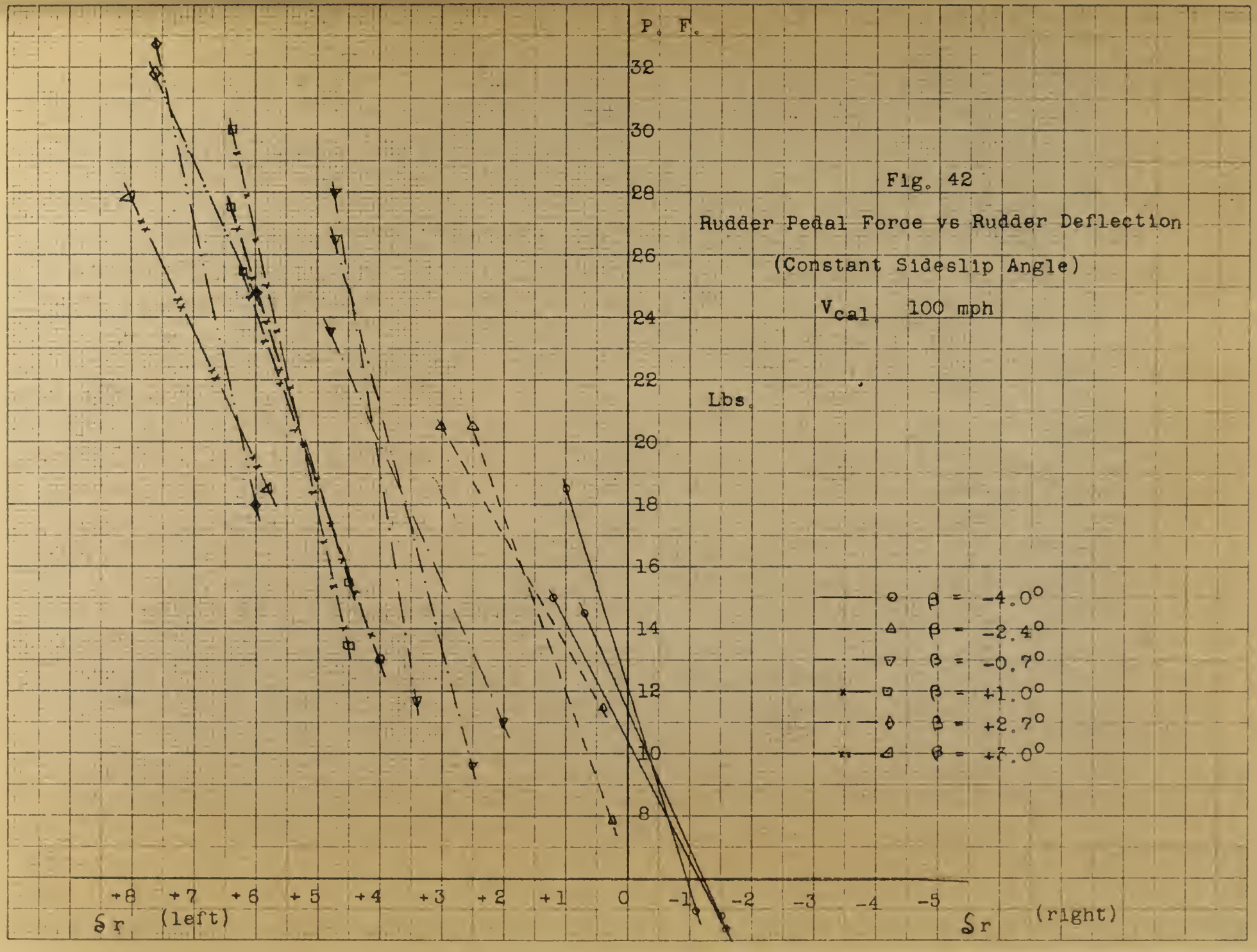

Fig. 42

Rudder Pedal Force vs Rudder Deflection

(Constant Sideslip Angle)

V_{cal} 100 mph

Fig. 43

Rudder Pedal Force Vs Sideslip Angle

(Constant Rudder Deflection)

$V_{cal.}$ 100 mph

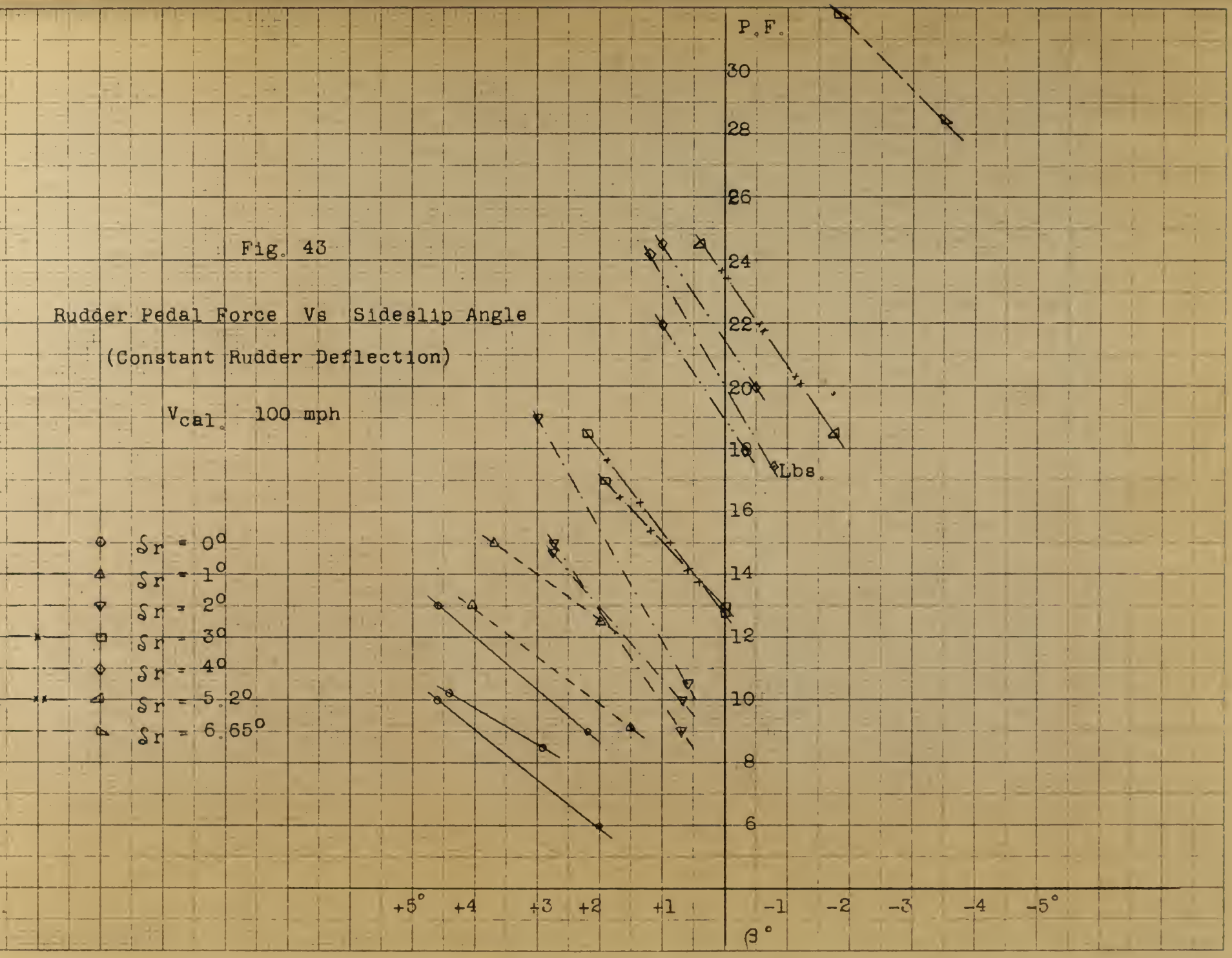

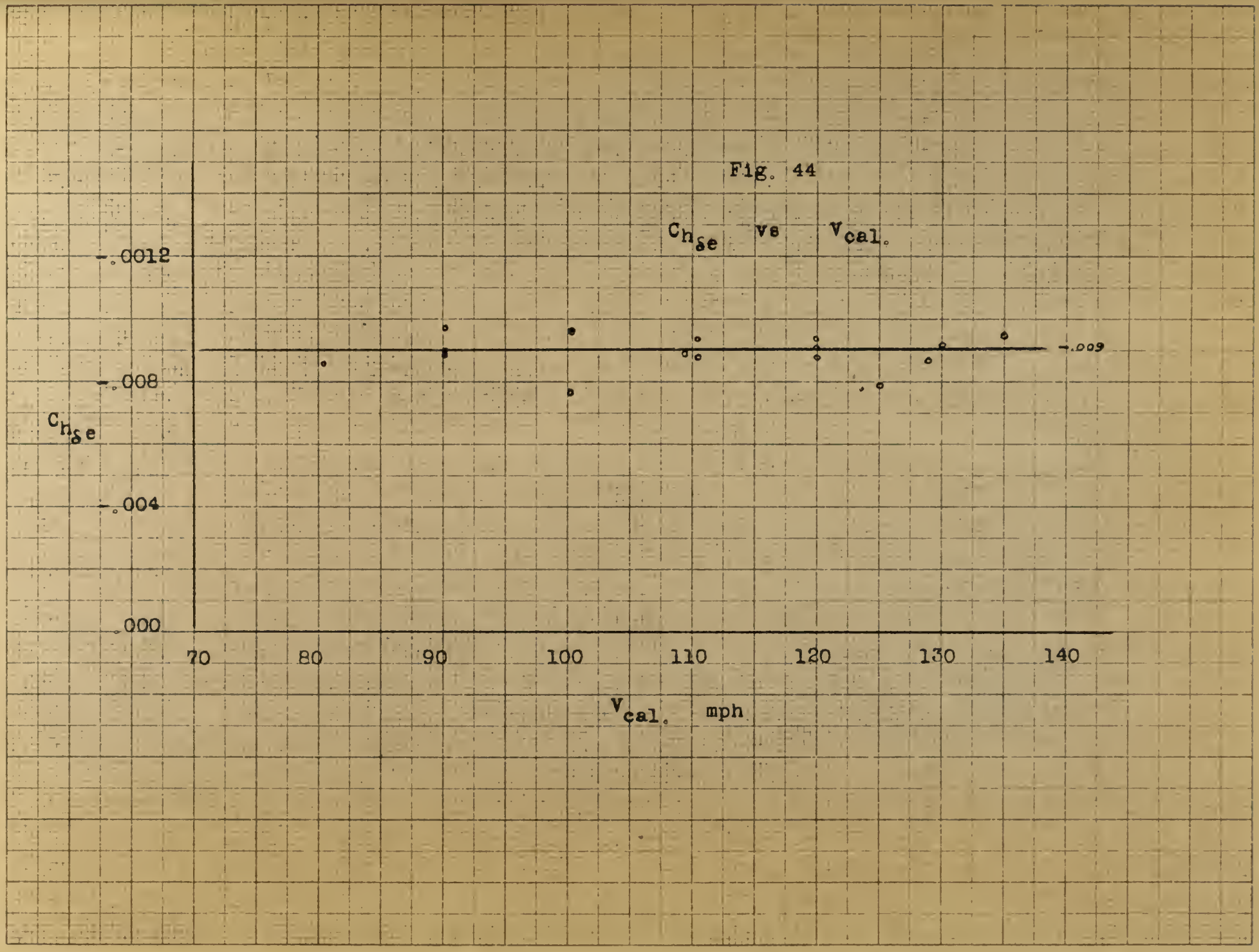
Fig. 44
$C_{h_{\delta e}}$ vs $V_{cal.}$
-.0012
-.008
-.004
.000
-.009
$C_{h_{\delta e}}$
70
80
90
100
110
120
130
140
$V_{cal.}$ mph

Fig. 45

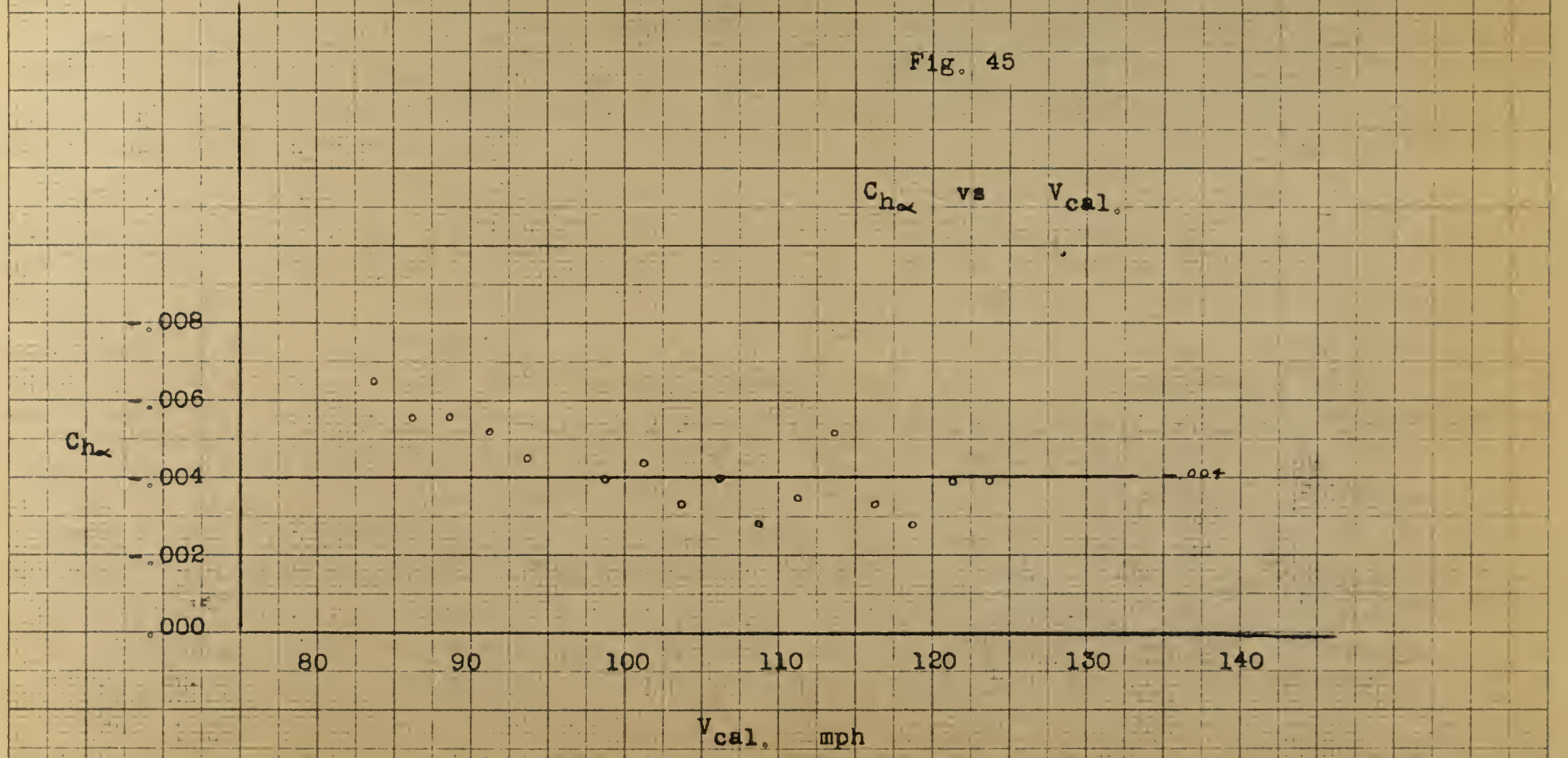
C_{h_α} vs $V_{cal.}$
-.008
-.006
C_{h_α}
-.004
-.002
.000
80
90
100
110
120
130
140
$V_{cal.}$ mph

Fig. 46

$C_{h_{sr}}$ vs β

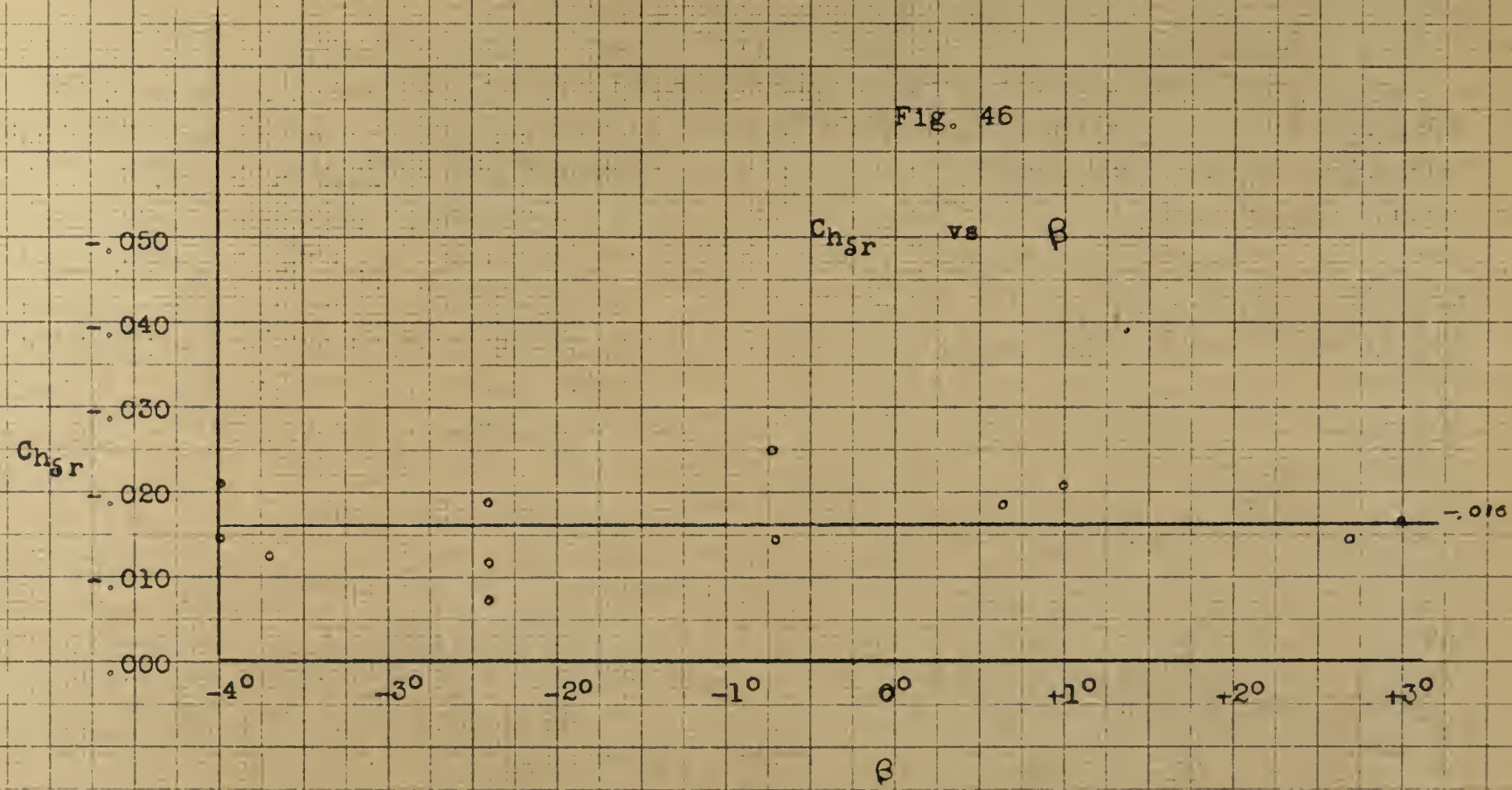

Fig. 47

C_{h_β} vs δ_r